Functional Genomics and Proteomics
National Centre for Biomolecular Research
Faculty of Science Masaryk University

CEITEC

Protein characterization by mass spectrometry

C7250

Part V

Zbyněk Zdráhal

RG Proteomics, CEITEC-MU
Proteomics CF, CEITEC-MU
NCBR FS MU
zdrahal@sci.muni.cz

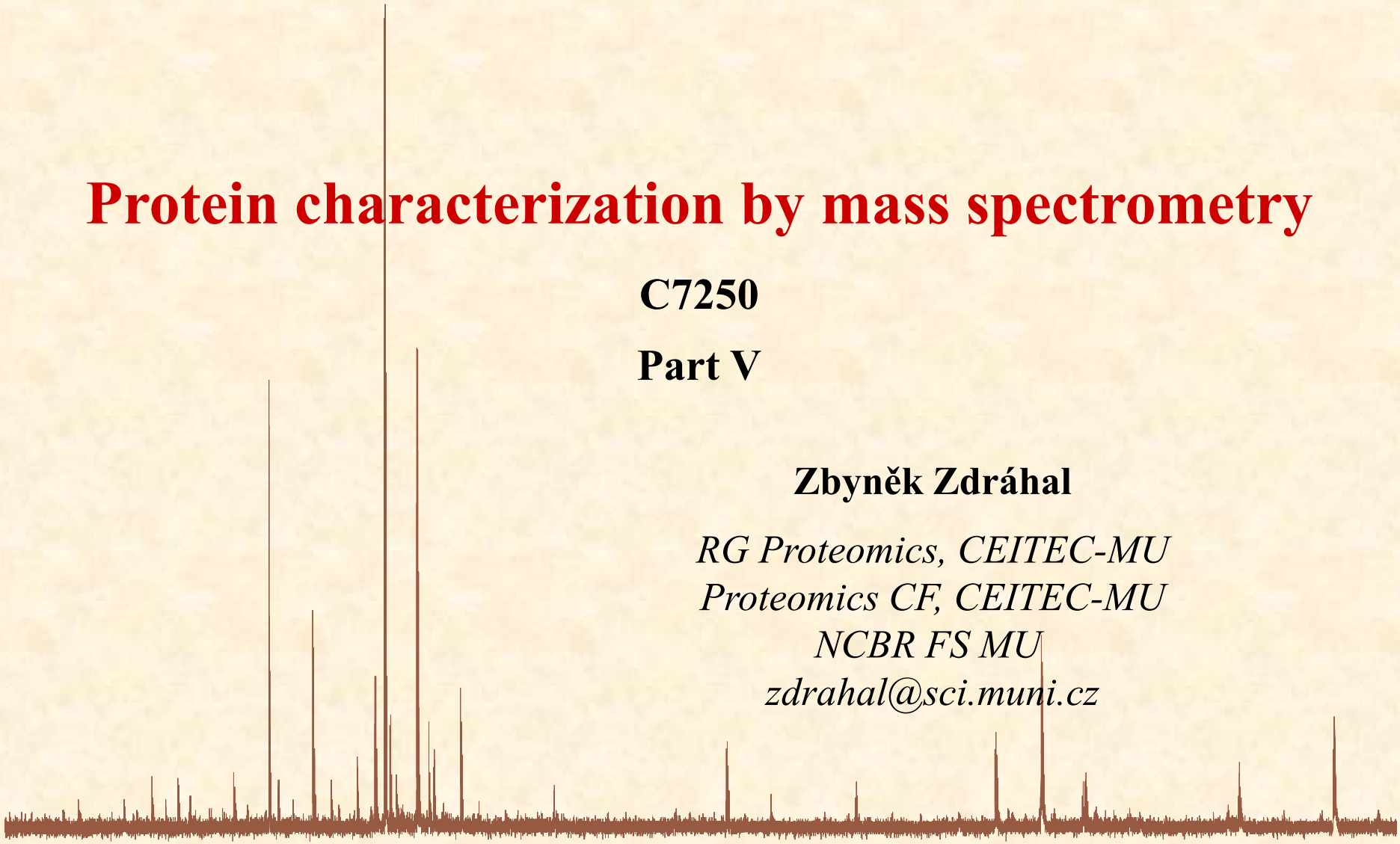

Proteomic MS applications

C7250

Assessment of products of synthesis

MALDI-MS

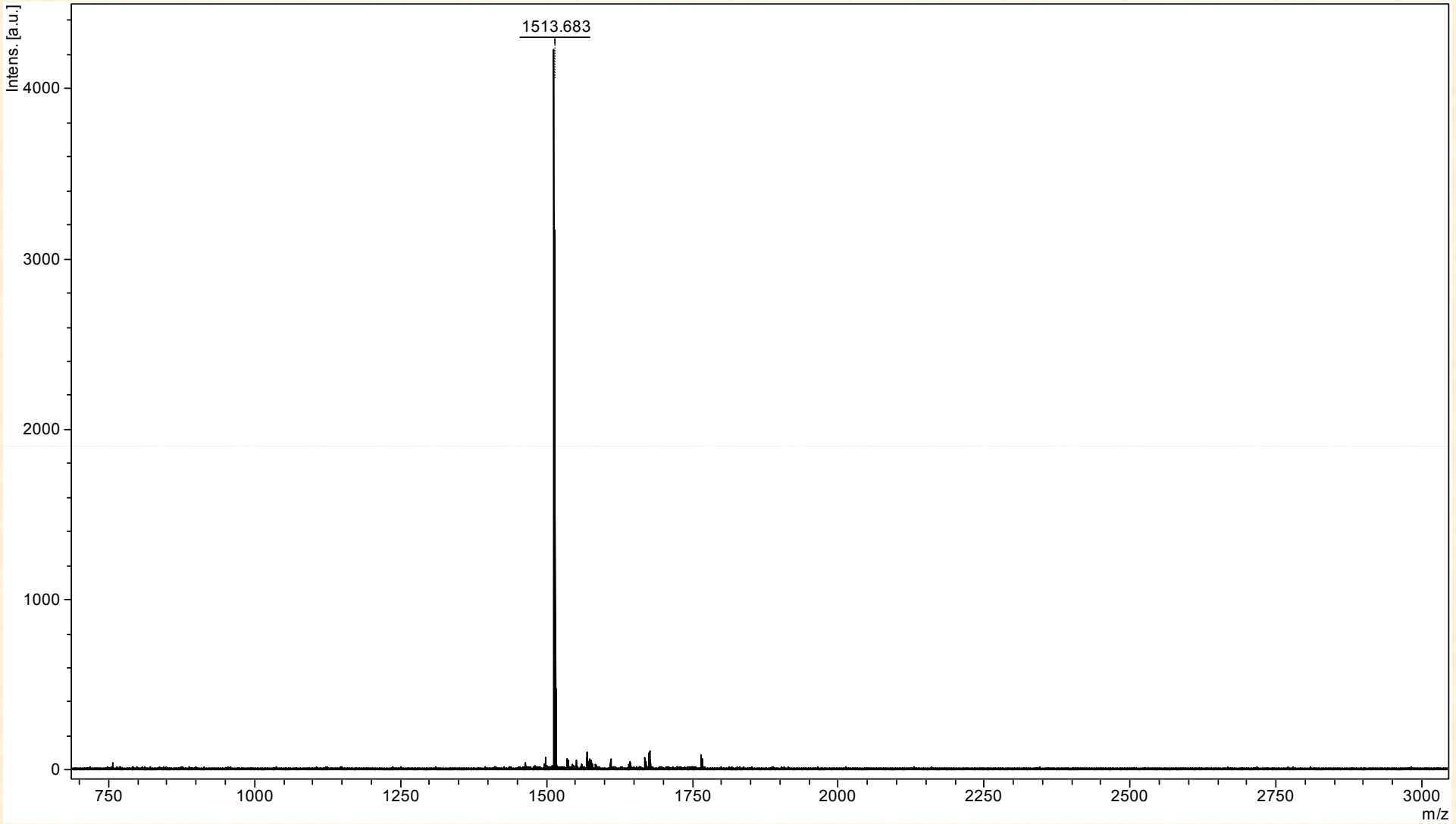

Assessment of reaction course

Modified BSA *vs.* std. BSA (≈ 5 pmol)

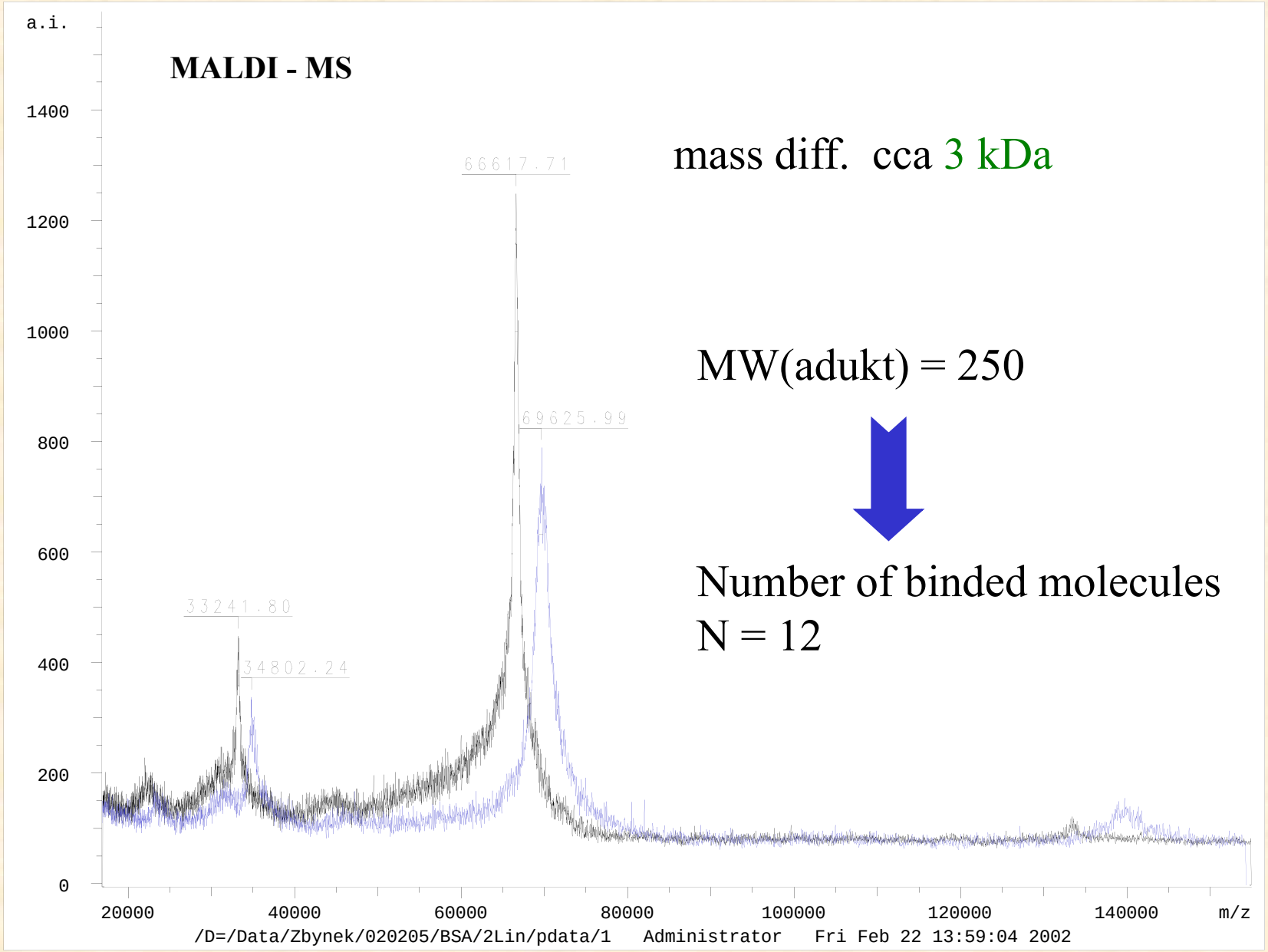

mass diff. cca 3 kDa

MW(adukt) = 250

Number of binded molecules
N = 12

„Evolution is strictly prohibited in this district“

MALDI-MS profiling

Identification of microorganisms by MALDI-MS

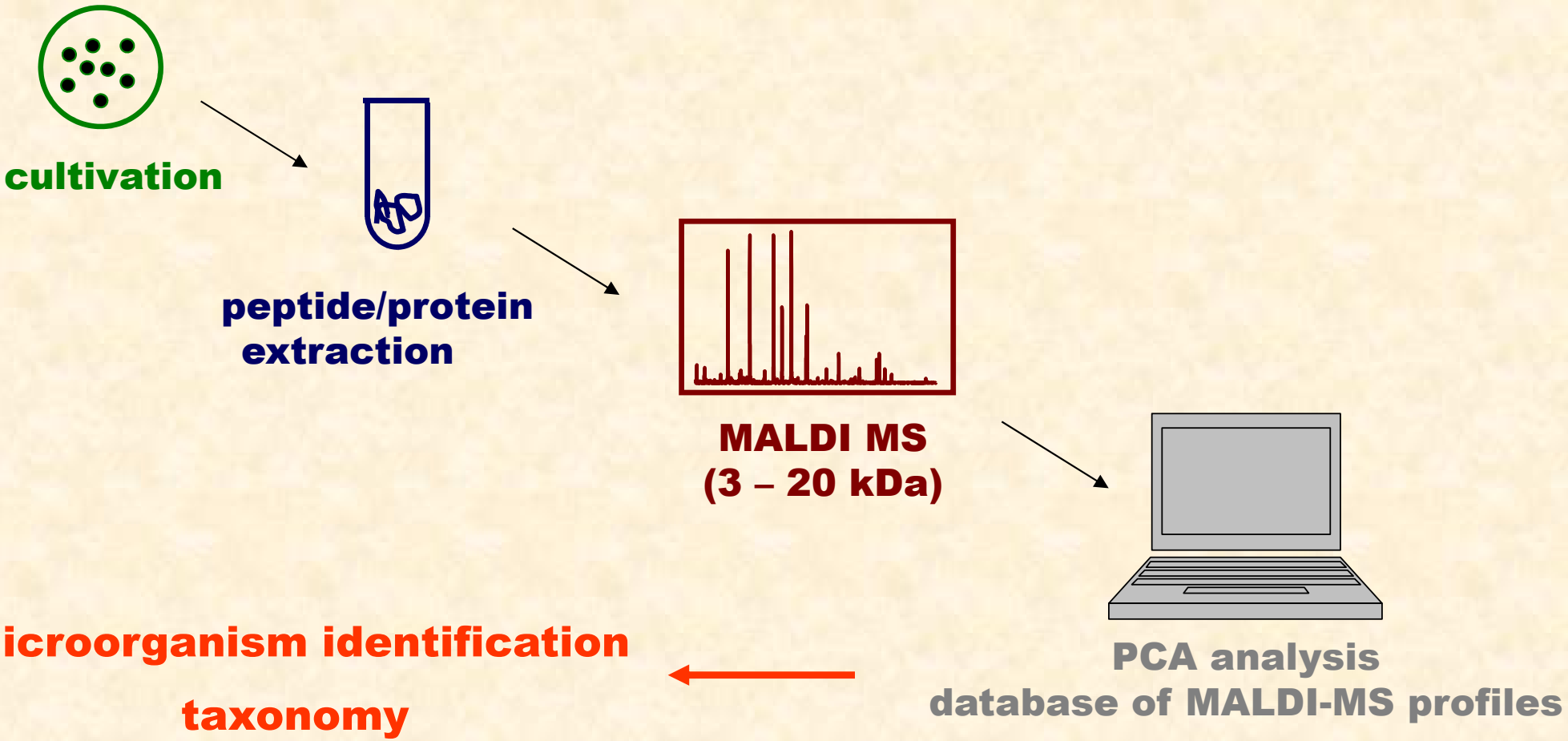

MALDI-MS spectra (profiles) of selected bacteria

C7250

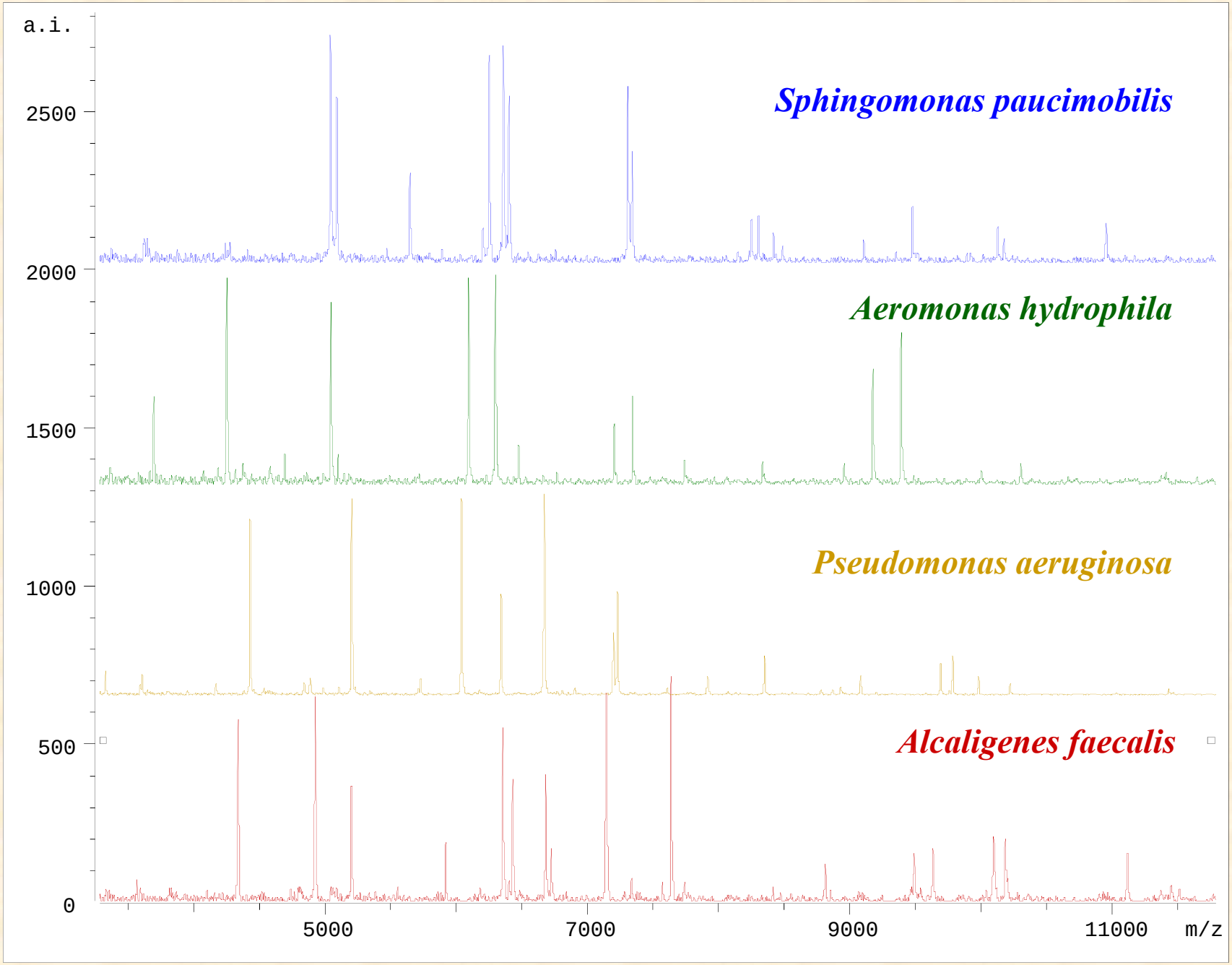

Graphical expression of MALDI-MS bacteria profile similarity

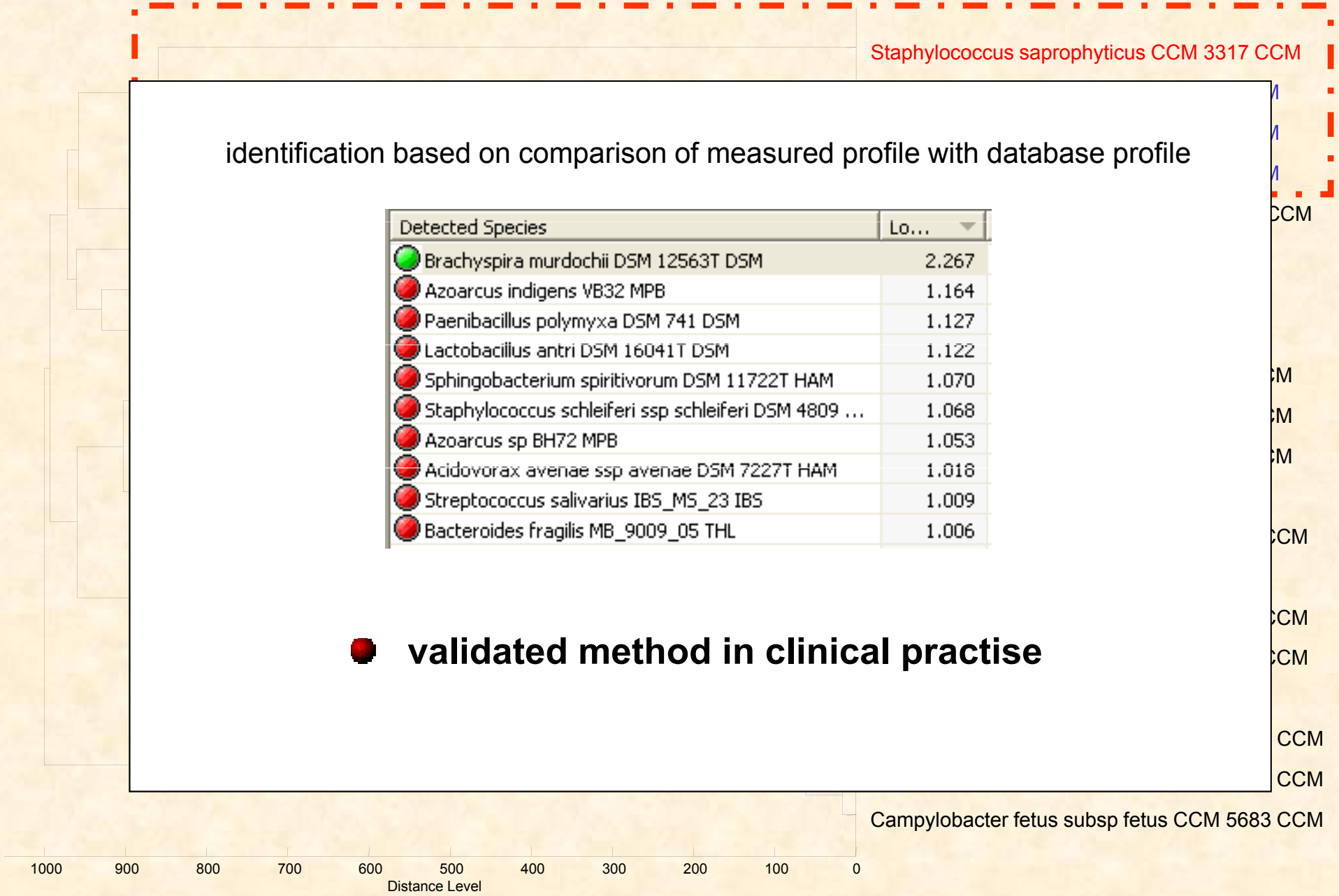

L. Tvrzová, A. Teshim, I. Sedláček, M. Lexa, A. Voráč, O. Šedo,, A. Kostrzewa, T. Meier

MALDI-MS profiling of beer

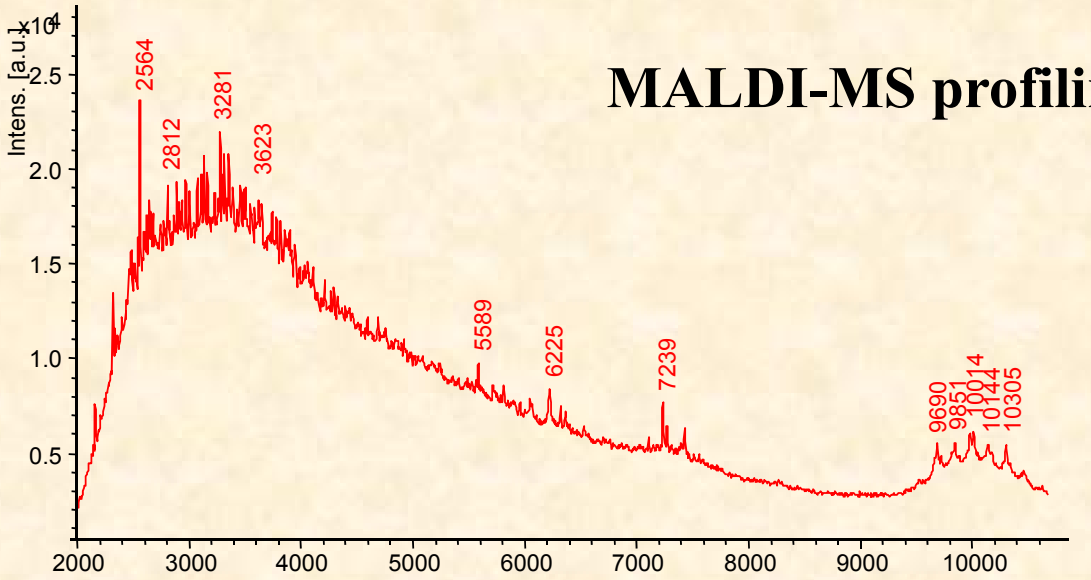

MALDI-TOF MS fingerprint containing proteins

cooperation with FCH BUT Brno
prof. Márová

MALDI-MS profiling of spider venoms

Z. merlijni

- evolution of food specialisation in spiders
- species adaptations
- ant-eating spiders

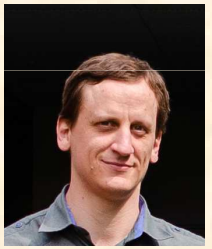

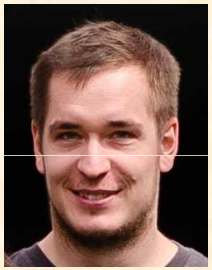

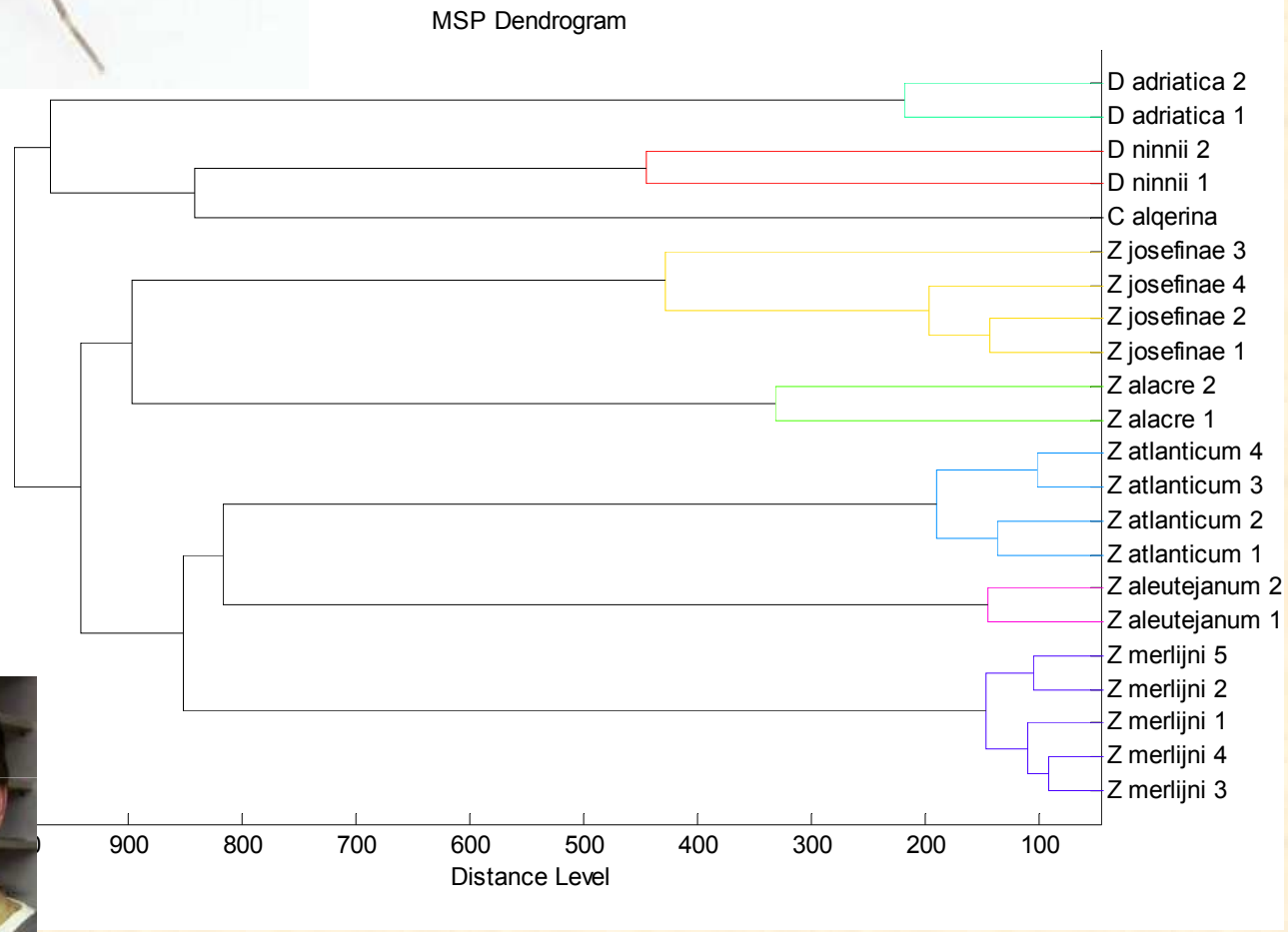

cooperation with prof. Pekar, FS MU

Pekár S. et al., J. Anim. Ecol., 81 (4), 838-848 (2012)
Bočánek O. et al., Toxicon, 133, 18-25 (2017)
Pekár S. et al. Mol. Ecol., 27 (4), 1053-1064 (2018)

MALDI-MS profiling–early detection of diseases

C7250

(peptide profiling, pattern profiling)

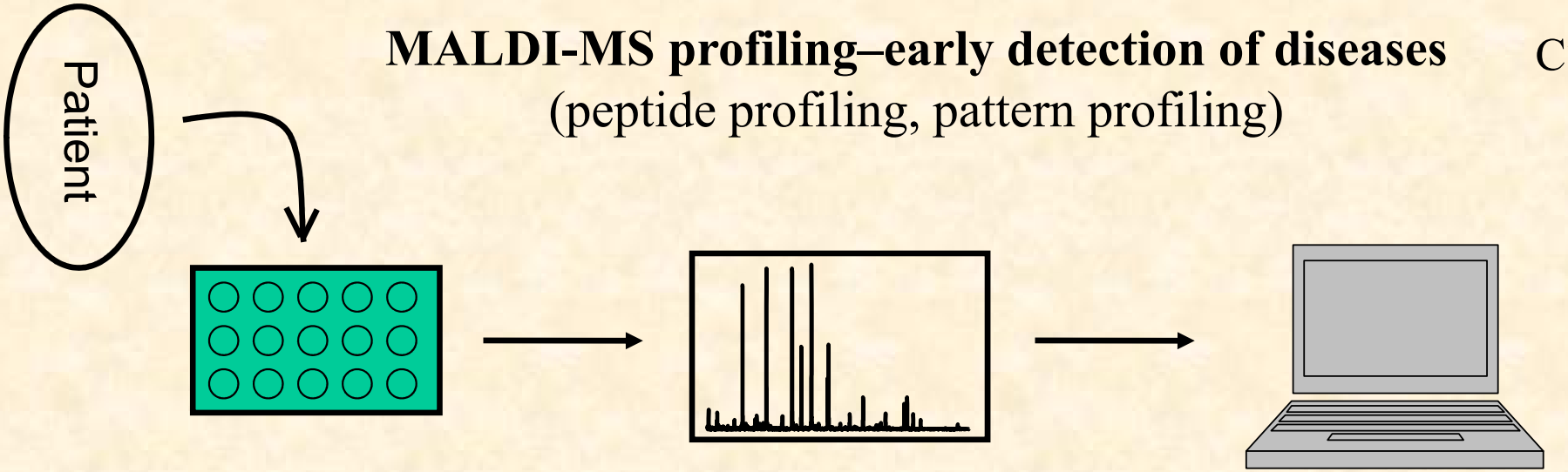

no or minimal sample prep
(ionex, IMAC, affinity sorbents)

MALDI MS, SELDI MS (3 – 20 kDa)

profile analysis

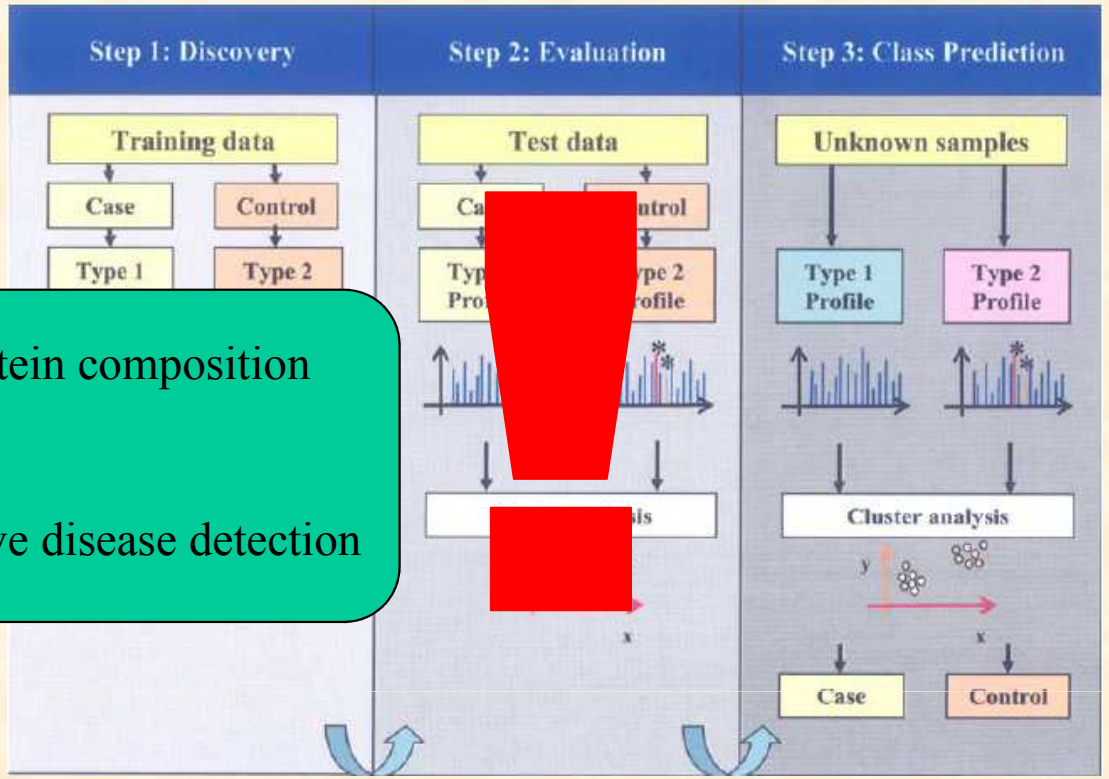

- high number of factors influencing protein composition
  not related with diagnosed disease
  high profile variability
- no strict limits for clear positive/negative disease detection

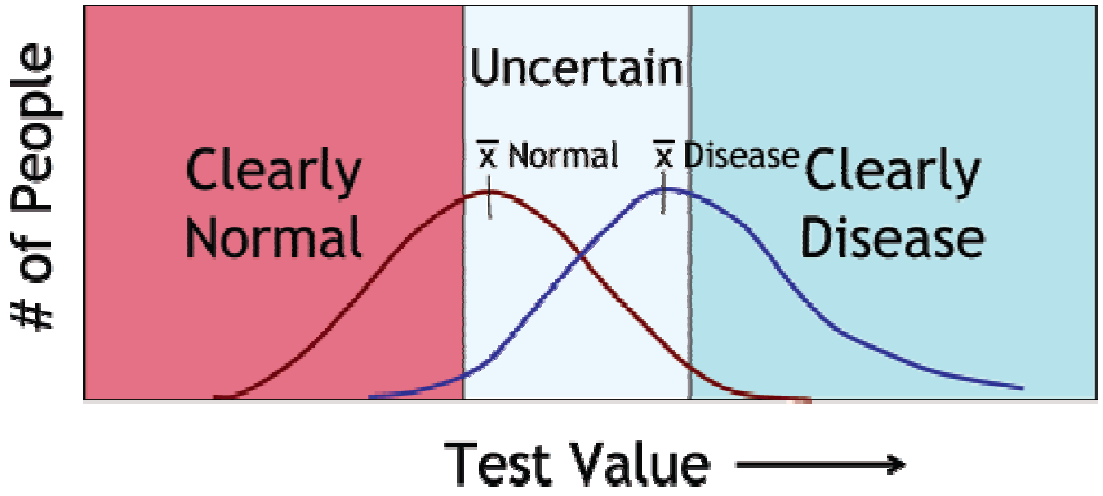

J. LaBaer et al., J. Proteome Res., ***4*** *(4) 1053-1059 (*2005).

M. Ehmann et al., Pancreas, ***34*** *(2) 205-214 (*2007).

MS-based approaches for biomarker searching

direct MS analysis
(MALDI MS, SELDI MS)

Pattern profiling

comparison of peptide (protein) profile of sample „healthy“ vs. patient
(bez identifikace, statistická analýza)

early disease detection

biomarker specifity!!!

biomarker identification

Separation
GE. LC

comparison of protein (peptide) content of sample „healthy“ vs patient

MS
MS/MS

identification of differentialy regulated proteins

specific antibody
Immunodetection
SRM, SWATH/Protein arrays

N-Glycan profiling of lung adenocarcinoma in patients at different stages of disease

C7250

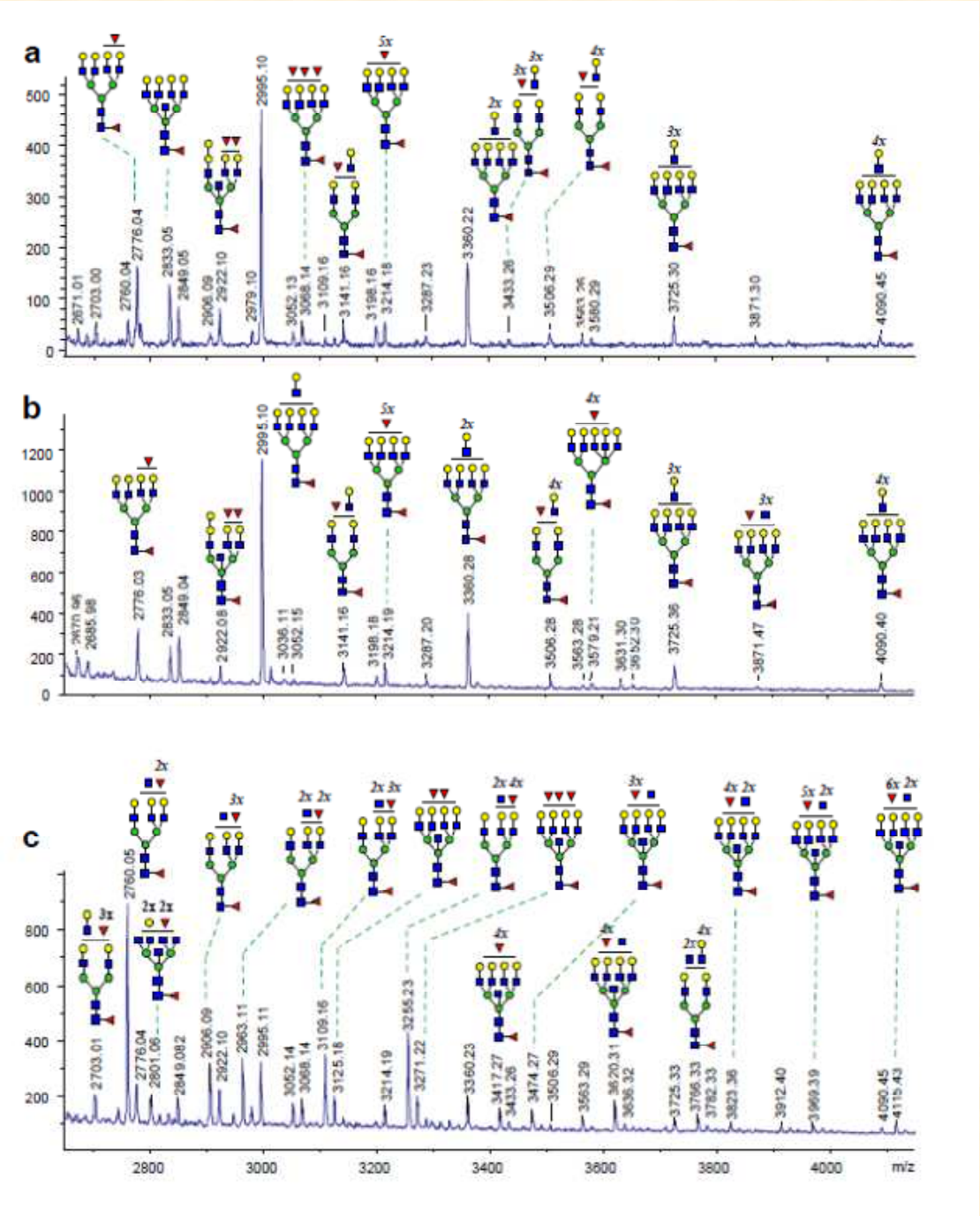

Detail of MALDI-MS spectra (m/z range of 2650-4150):

a) P1 (stage IB/grade1)
b) P7 (stage IIA/grade4)
c) P13 (stage IIIA/grade2)

MALDI-TOF-MS spectra of N-glycans after desialylation

Man; Gal; GlcNAc; Fuc

Lattová E. et al., Modern Pathology (2020) 33:1146–1156


BERLINBEAIRBUS

Relative quantification by MS

- **isotopically labeled tag approaches**
  (comparison of limited number of samples, up to 10)

protein quantification

replica 1

replica 2

replica 3

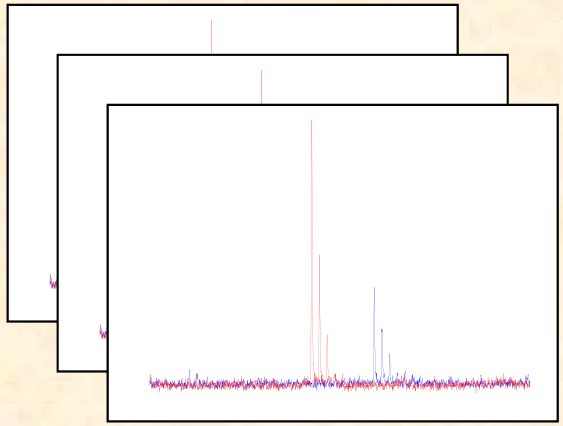

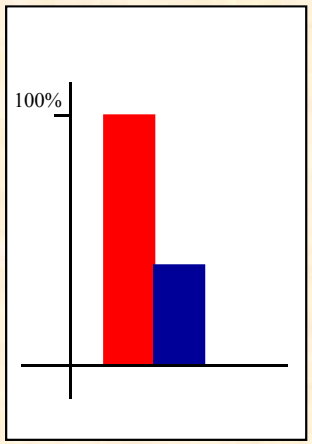

- **label-free approaches**
  (comparison of unlimited number of samples, lower accuracy)

Targeted quantification of selected proteins by MS

- MRM (SRM), PRM

Characterization of proteome changes
differential (expression) proteomics

image analysis of 2-D gels
LC-MS/MS of selected spots with different intensity

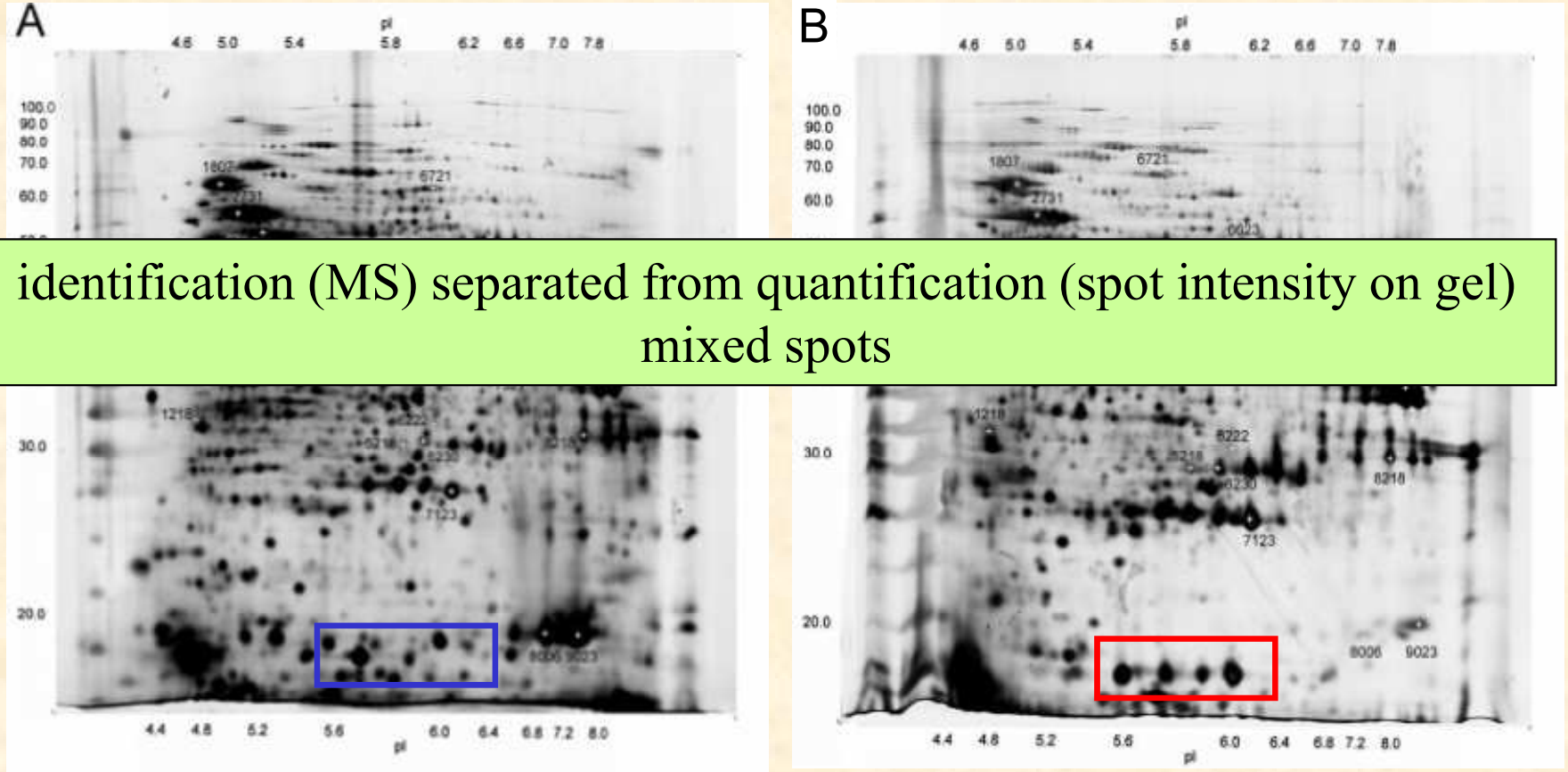

identification (MS) separated from quantification (spot intensity on gel)
mixed spots

Acidithiobacilus ferrooxidans grown on ferrous iron (A) and elemental sulfur (B)

cooperation with Department of Biochemistry, FS MU
P. Bouchal et al., Proteomics 2006, *6,* 4278–4285.

Search for marker proteins for chicken salmonella infection relative quantification

control

infected

gut wall sample

protein isolates

tryptic digestion

reductive alkylation

LC-MS/MS

data processing

- identification more than 2300 protein
- quantification for more than 1900

Accession	Description	infected/ control
363741657	PREDICTED: syntenin-2-like [Gallus gallus]	41.032
118095649	]	34.036
4927286		33.575
112491068		30.221
56118294	ribonuclease homolog precursor [Gallus gallus]	25.497
363741459	PREDICTED: protein-glutamine gamma-glutamyltransferase E [Gallus gallus]	24.786

clarifying of mechanisms of molecular processes

search for marker proteins for early detection

confirmation by real-time PCR

cooperation with VRI Brno

Matulova M. et al., Vet. Res., 44:37 (2013)

Characterization of the extent and dynamics of translational regulation during tobacco male gametophyte development and the subsequent functional progamic phase

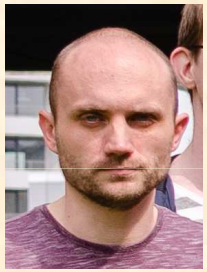

the **three types of mRNA-containing ribonucleoprotein particles**:

- **POL** - translating polysomes
- **RNP** - free ribonuclear particles
- **EPP** - long-term storage EDTA/puromycin-resistant particles

six developmental stages

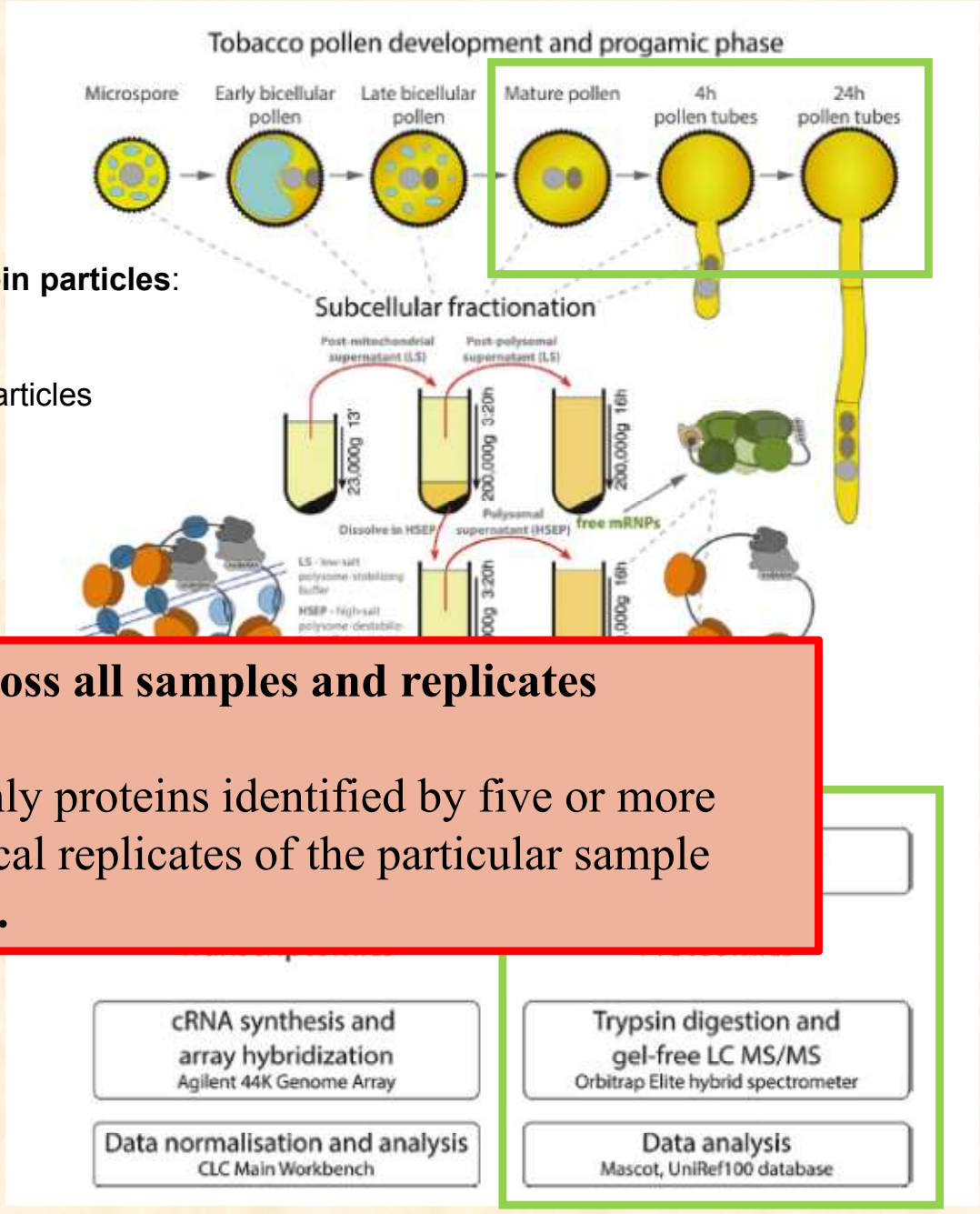

- **9317 protein groups identified across all samples and replicates**
- **2,089 for quantitative analyses** (only proteins identified by five or more peptides in all biological and technical replicates of the particular sample were considered as reliably present)**.**

Hafidh S. et al., Plant Physiol., 178 (1), 258-282 (2018)

Characterization of the extent and dynamics of translational regulation during tobacco male gametophyte development and the subsequent functional progamic phase

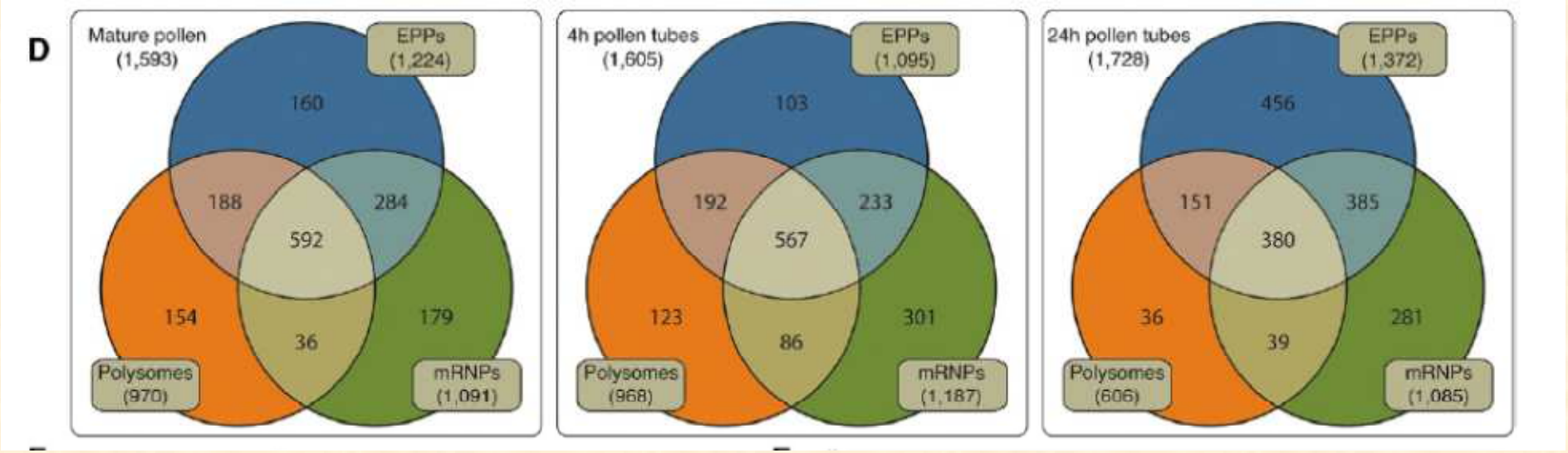

Overall abundance of PABP transcripts

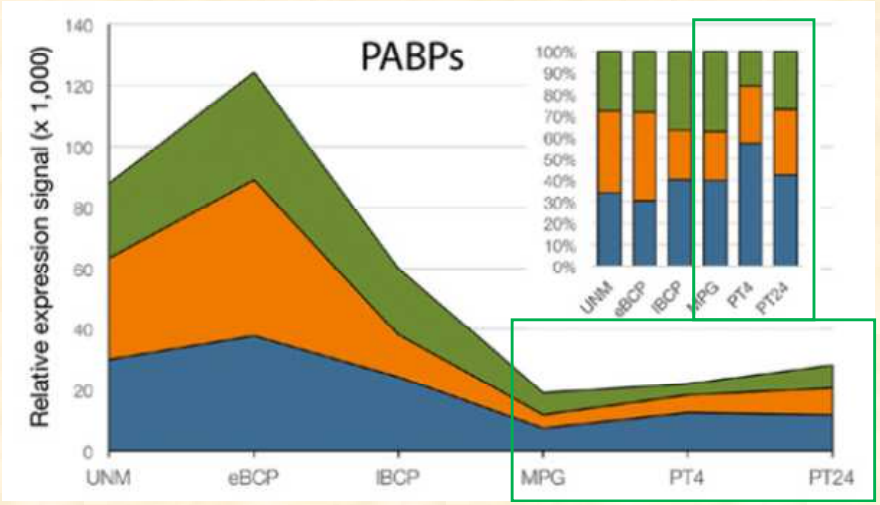

Dynamics of seven protein groups associated with PABPs

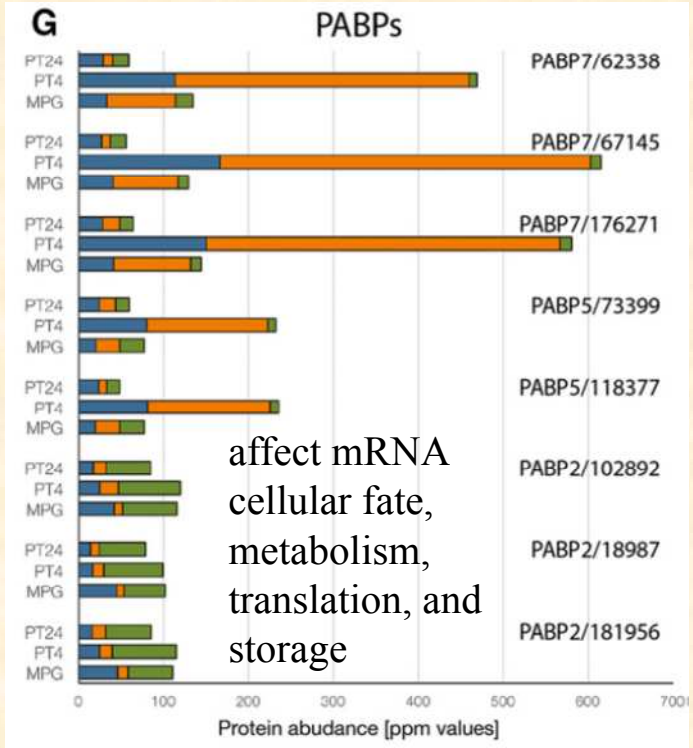

affect mRNA cellular fate, metabolism, translation, and storage

Hafidh S. et al., Plant Physiol., 178 (1), 258-282 (2018)

The quantitative and condition-dependent *Escherichia coli* proteome

22 different growth conditions in biological triplicates.

(i) growth on minimal media with an excess of different carbon and energy sources
(ii) growth in glucose-limited chemostat cultures with varying growth rates,
(iii) growth on glucose excess with different stress conditions,
(iv) growth on complex medium, and
(v) 1 and 3 d into stationary phase.

cellular protein concentrations for **55% of predicted *E. coli* genes** (>2,300 proteins)

41 proteins related to glycolytic pathway, tricarboxylic acid cycle enzymes and others was selected to absolute quantification

The **concentration range** of the 41 proteins covered more than **four orders** of magnitudes ranging from around **92,000 to only 2 copies per cell**.

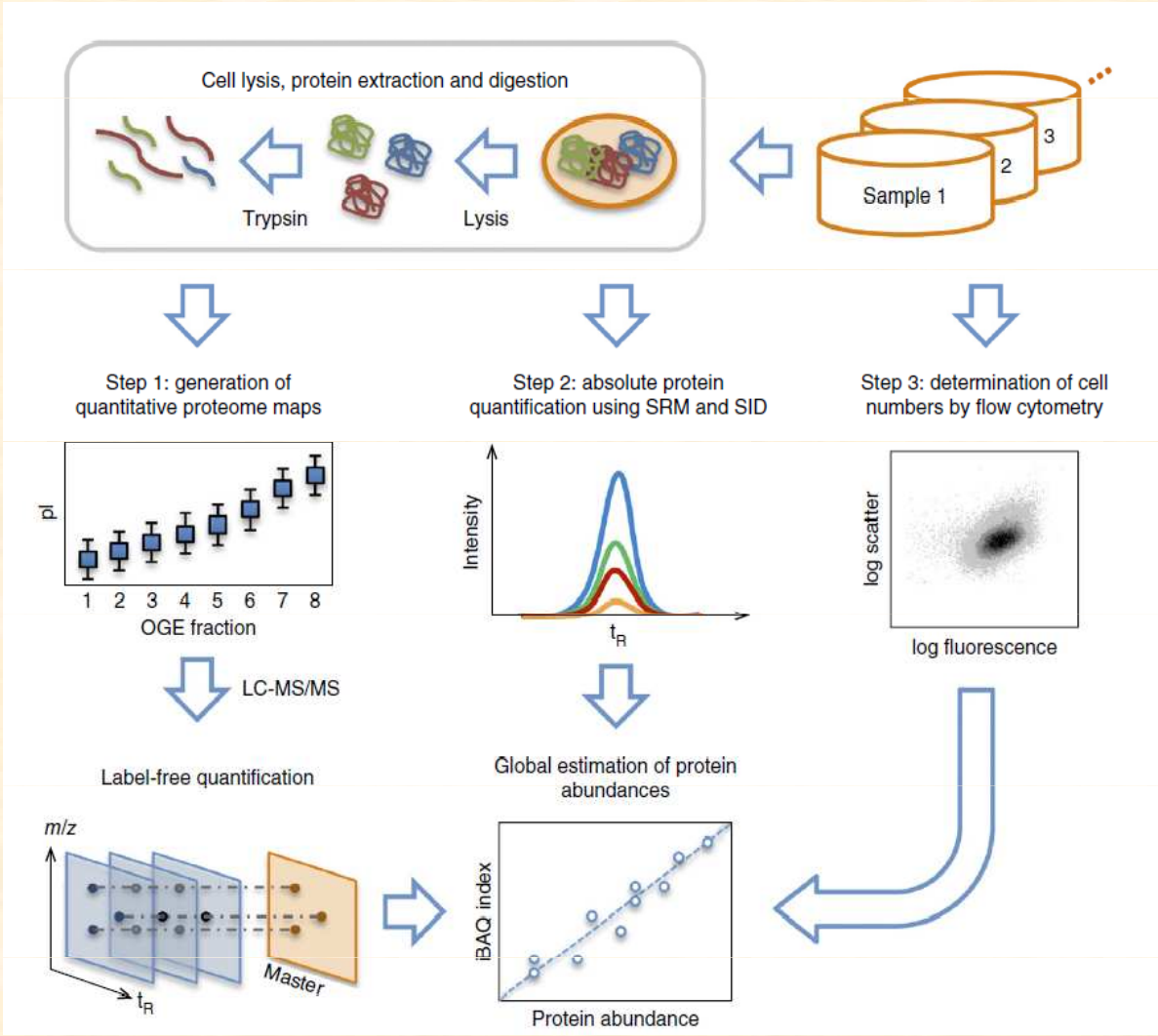

*Schmidt A., Nature Biotechnol., **34** (2016), 104 – 110*

Comparison of human cancer cell line proteome and transcriptome

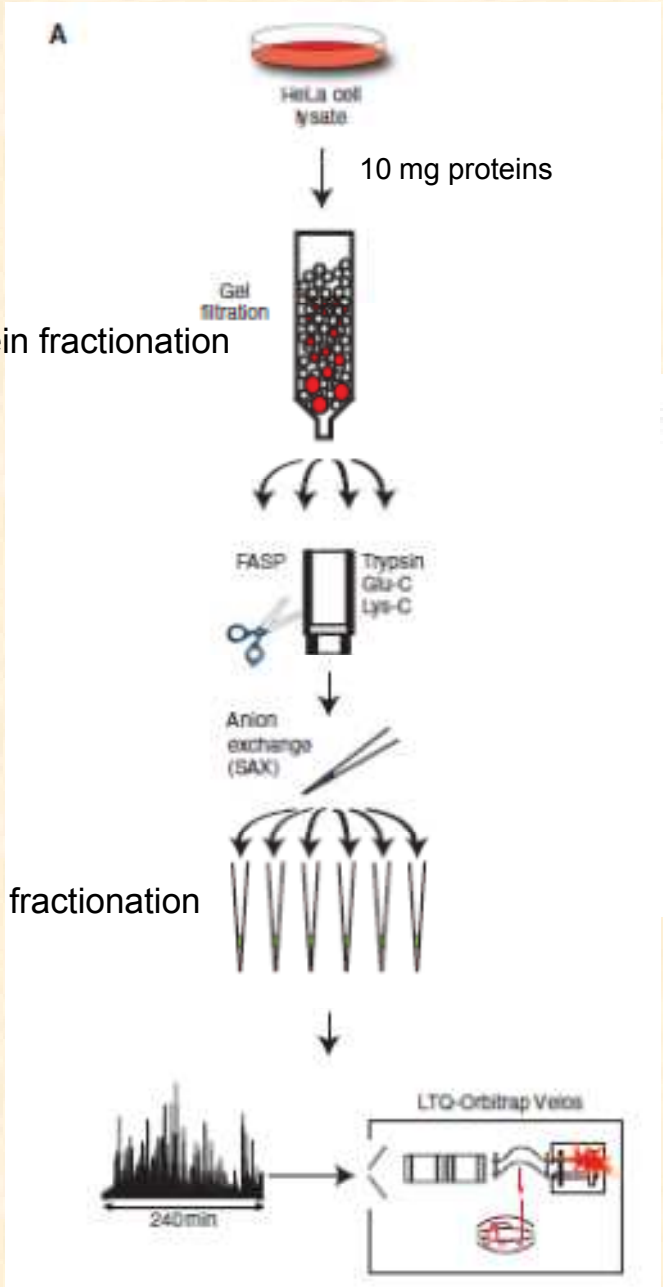

126 frakcí

72 frakcí

B

Experiment	Proteins	Peptides	MS measurement time
Exp 1	*10 596*	*187 006*	*21 days*
Exp 2	10 255	163 784	12 days

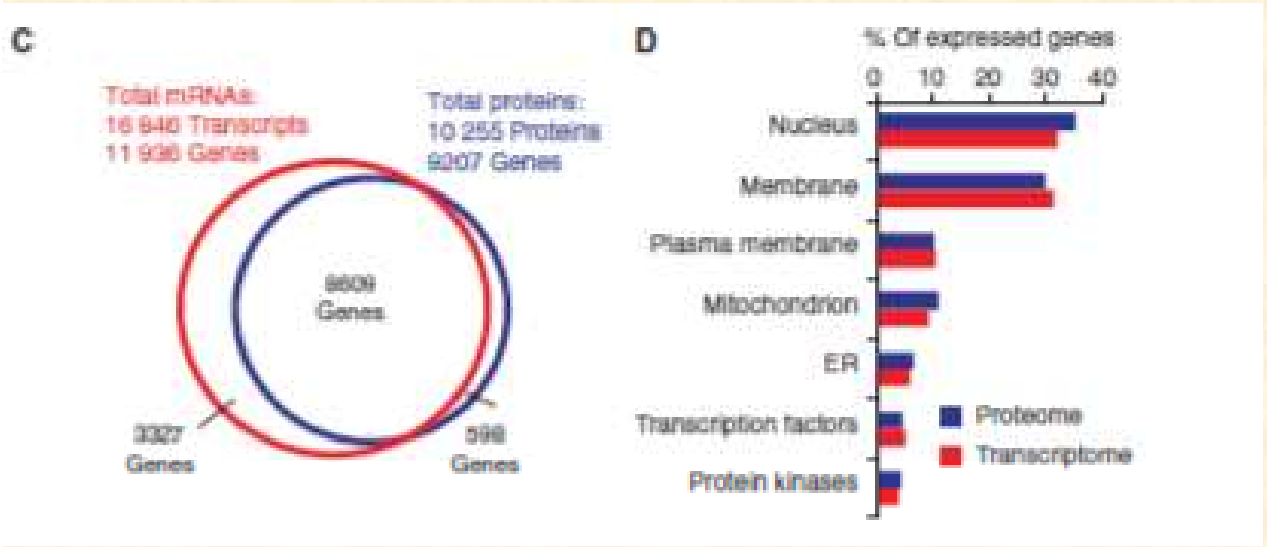

*N. Nagaraj et al., Mol. Syst. Biol., 7, 548 (*2011).


701

Targeted analysis of selected protein/PTM

Schematic workflow of a constrained SRM assay

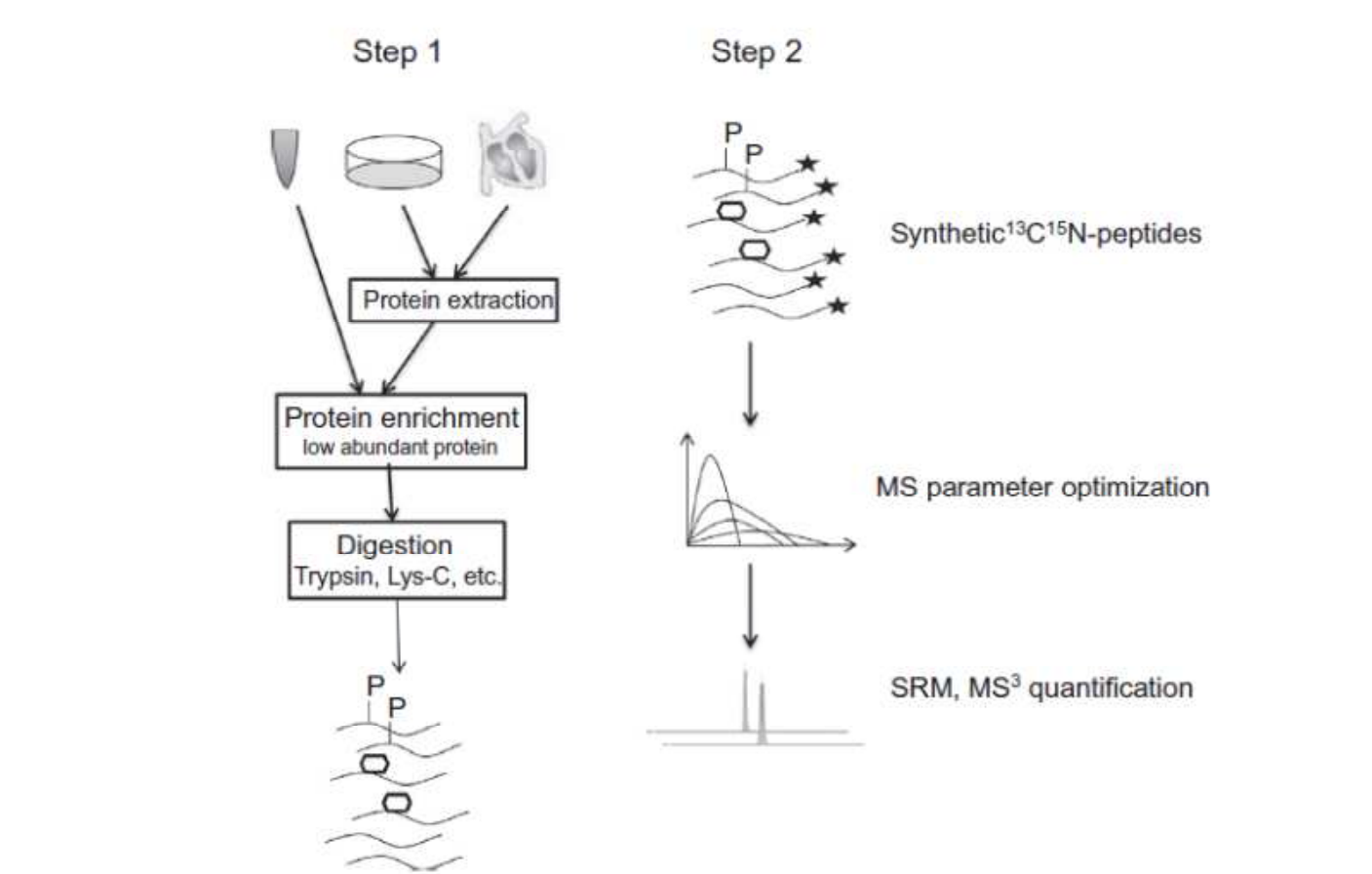

Step1: 1. Biological samples include body fluids (such as blood or saliva), cell lysate, and tissue. 2. PTM proteins and protein isoforms are extracted from cell lysate and tissue. 3. Protein enrichment methods are applied for less abundant proteins. 4. PTMs and protein isoforms are digested by enzymes, including trypsin, Lys-C, etc. 5. After digestion, modified, unmodified peptides, and peptides representing the whole protein are selected.

Step2: 1. Isotope-labeled peptides are synthesized to serve as internal standards for the post-translationally modified peptides, unmodified peptides, and peptides representing the whole protein. 2. Mass spectrometer parameters are optimized by using the synthetic peptides. 3. Isotopic labeled peptides are internal standards and spiked in the samples. PTMs and isoforms are quantified by SRM or MS3 assay.

Liu X., et al., Methods 61 (2013) 304–312

Targeted analysis of selected protein/PTM
SRM

IADPEHDHTGFLTEYVATR

IADPEHDHTGFLTEYVATR – 2x Phospho

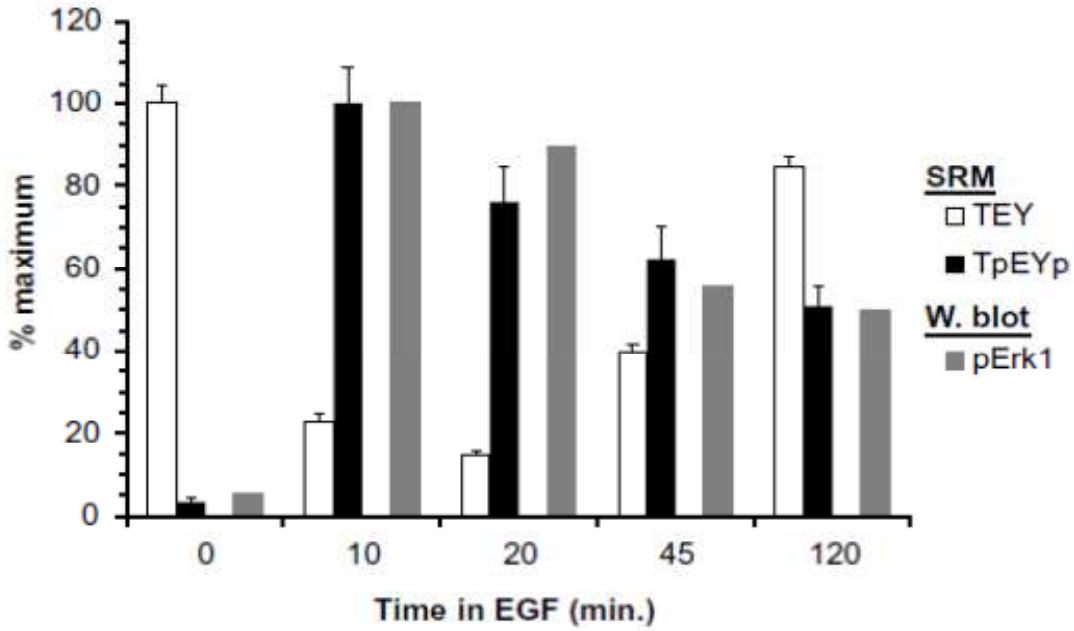

SRM and western blot assays show a similar **time-course of Erk1 phosphorylation** in response to EGF.

Liu X., et al., Methods 61 (2013) 304–312


G-ZAPM
COPYRIGHT JOHN GREGORY
AIRLINERS.NET

Phosphoproteome analysis – four fractionation approaches

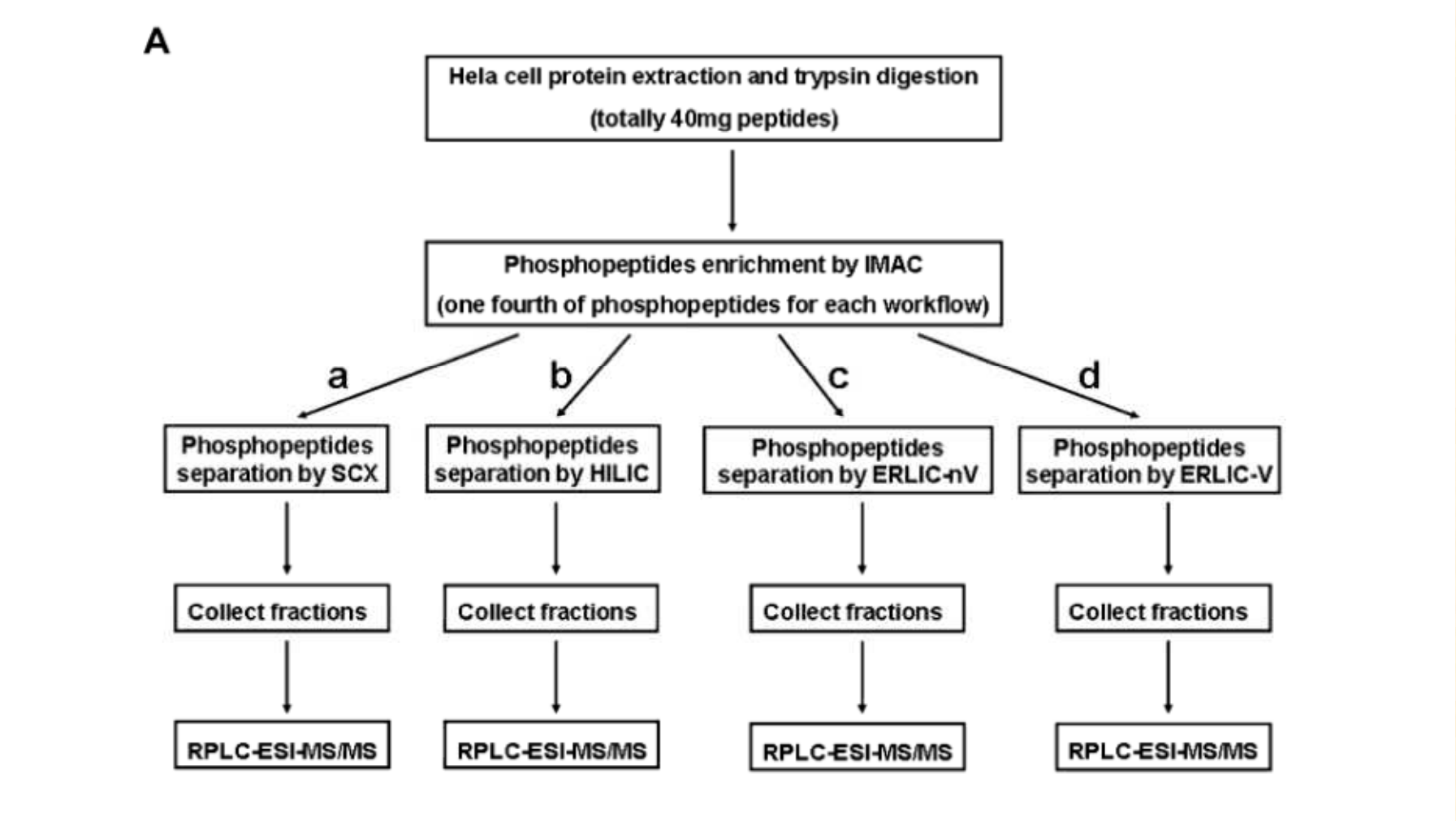

ERLIC - Electrostatic Repulsion-Hydrophilic Interaction Chromatography

Chen et al., J. Chromatogr. B, 879, 25 (2011)

Phosphoproteome analysis – four fractionation approaches

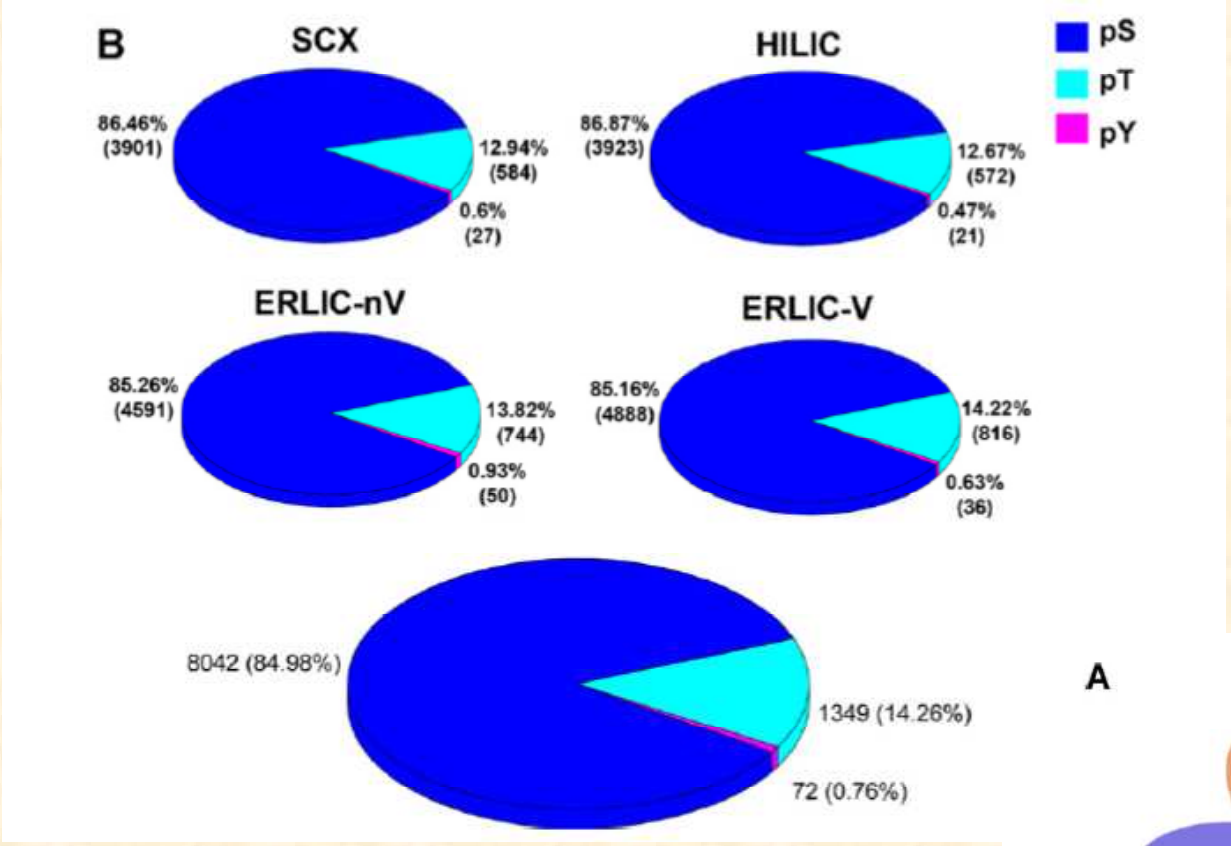

Each method – over 4000 phoshopeptides
In total – 9069 phosphopeptides – 9463 sites / 3260 proteins

Chen et al., J. Chromatogr. B, 879, 25 (2011)

Phosphoproteome analysis– quality and quantity

Porcine muscle
Postmortem changes

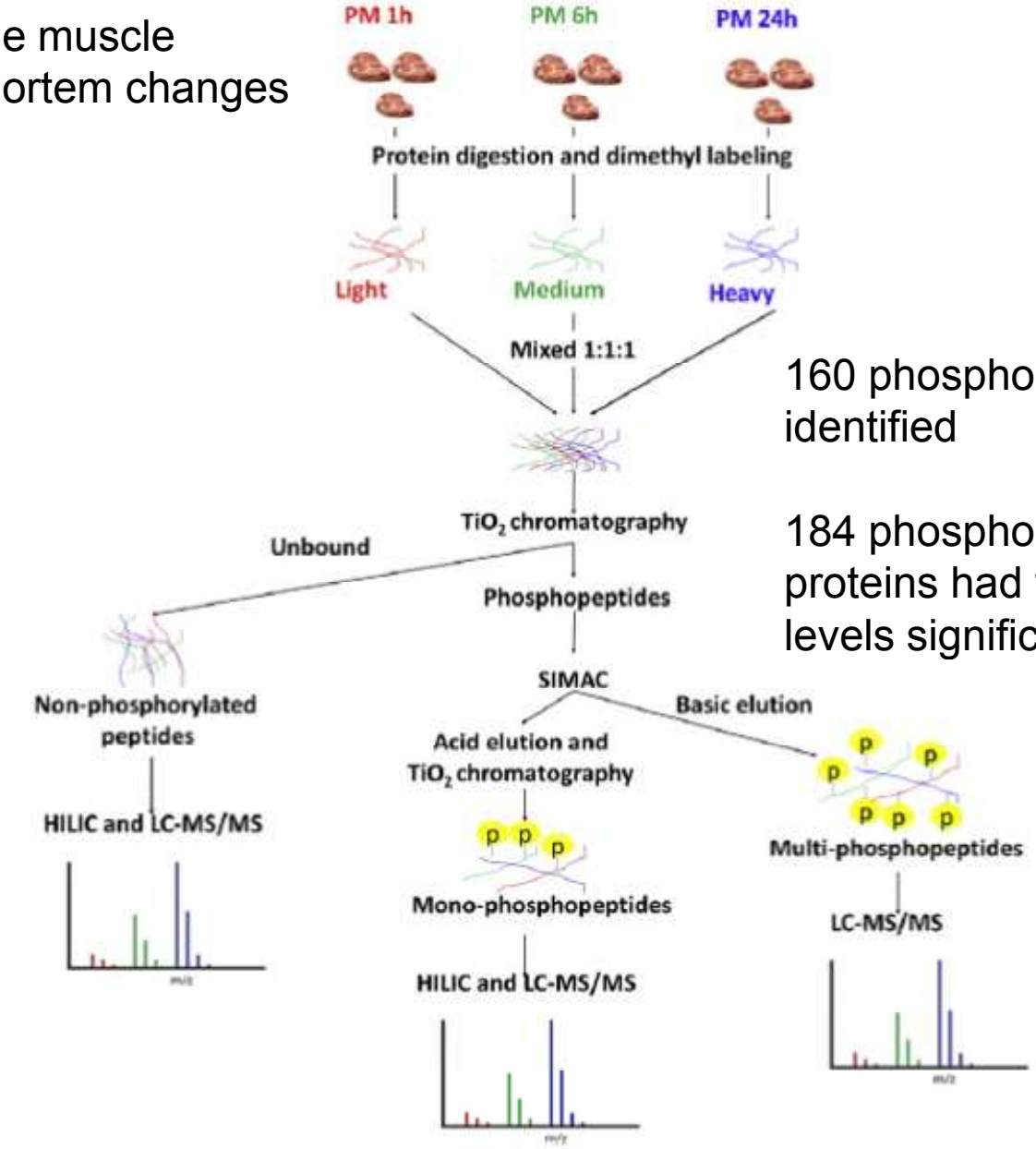

160 phosphoproteins with 784 sites identified

184 phosphorylation sites on 93 proteins had their phosphorylation levels significantly changed.

Huang et al., J. Proteomics, 106, 125 (2014)

Phosphoproteome analysis– quality

Comparison of identified peptides in replicas

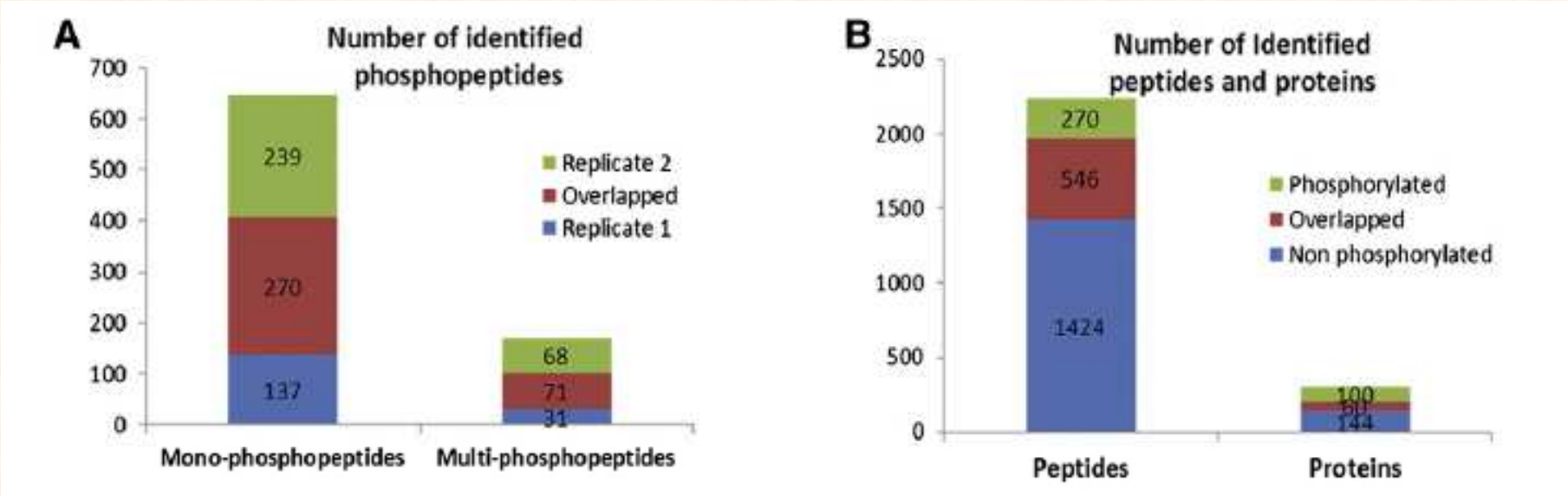

Huang et al., J. Proteomics, 106, 125 (2014)

Phosphoproteome analysis

Olsen J.V. et al., Sci. Signal., 3 (104) ra3 (2010)

- quantified 6027 proteins
- quantified 20,443 unique phosphorylation sites

- HELA cells
- SILAC labeling
- TiO_2 enrichment
- LC-MS/MS (Orbitrap)

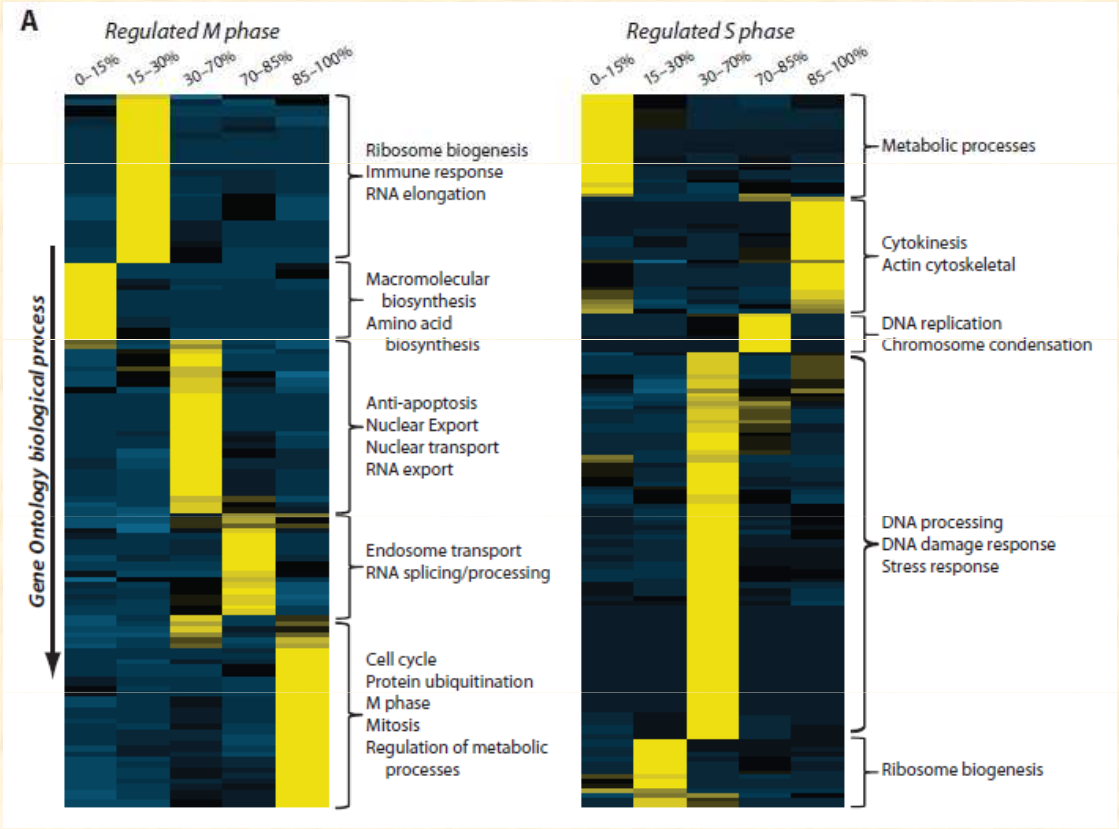

The panels show the phenotypic phosphoproteome comparison organized by GO biological process for mitotic (left) and S phase (right) cells. Proteins involved in metabolic processes have high-occupancy phosphorylation sites during mitosis, but low-occupancy sites during S phase (color scale: yellow, high overrepresentation; dark blue, high underrepresentation).


CEBU PACIFIC AIR.COM

Characterization of effect of histone deacetylase inhibitors

- to **establish a set of methods**

  - HDAC Fluorimetric Cellular Activity Assay Kit
  - MALDI-MS of N-terminal part of histones (after Glu-C digestion)
  - AUT-AU 2-D GE combined with LC-MS/MS analysis

Total HDAC inhibiton effect

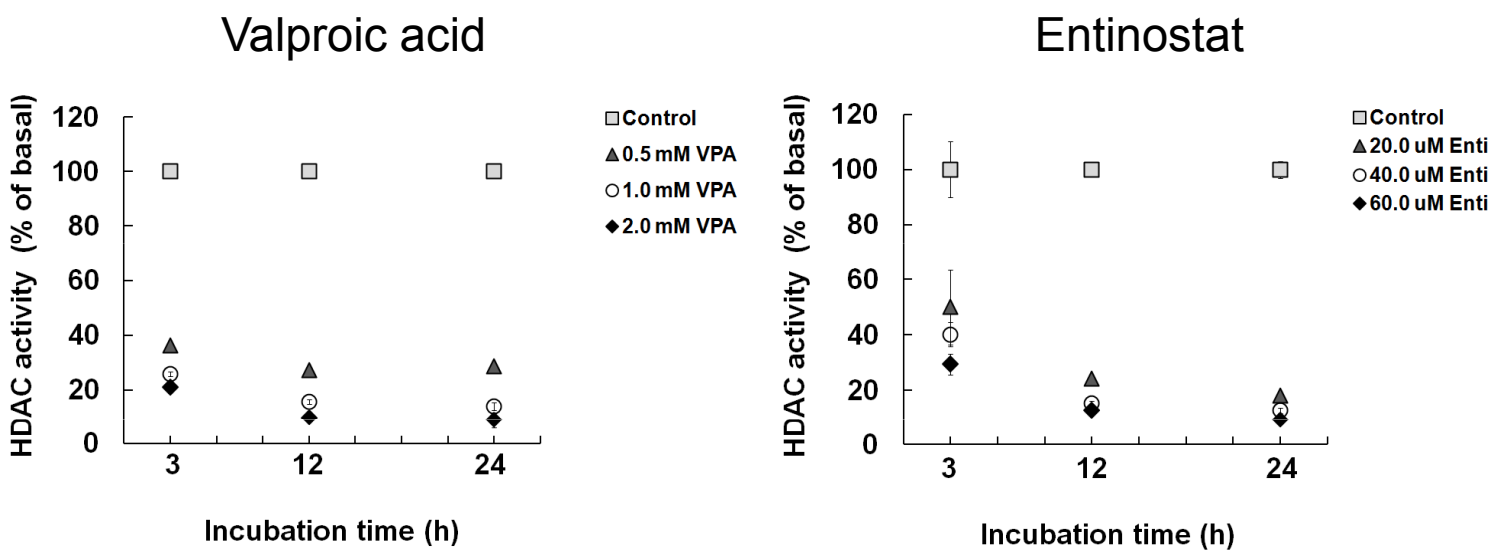

B-CLL MEC-1 cells

Činčárová et al, Mol. Biosyst. (2012)

Characterization of effect of histone deacetylase inhibitors

MALDI-MS of Histone H4 acetylated forms

N-terminal fragment (1-53 AA)

control

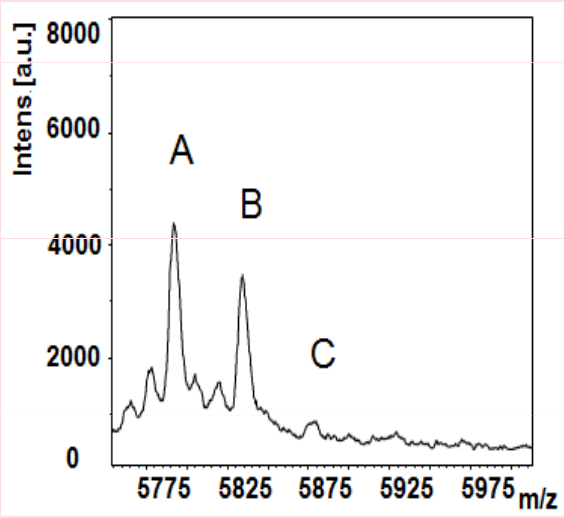

Valproic acid

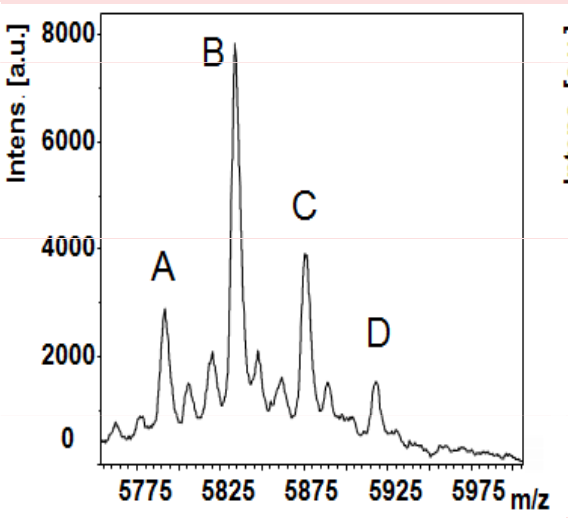

Entinostat

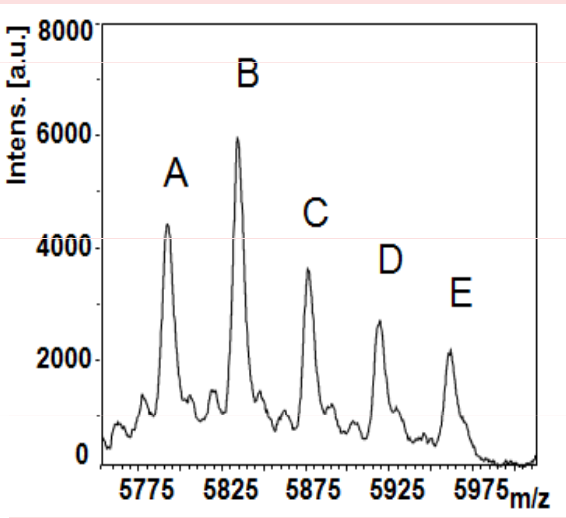

A → E 0 → 4 acetylations

Characterization of effect of histone deacetylase inhibitors

Changes of particular H4 acetylated forms *vs* inhibitor concentration

(24h treatment)

Valproic acid

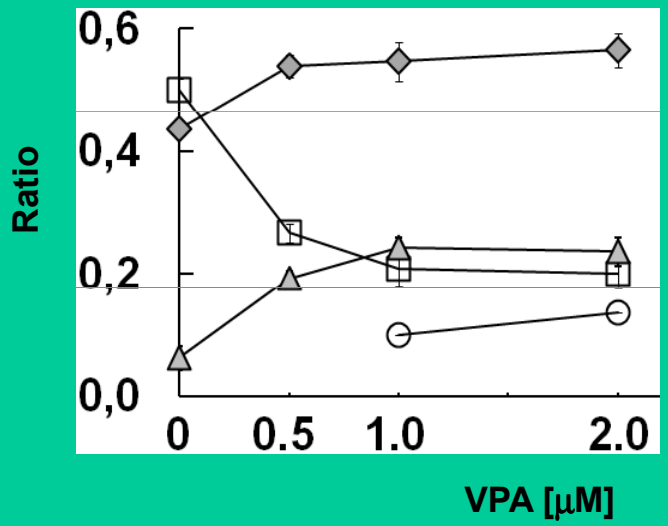

Entinostat

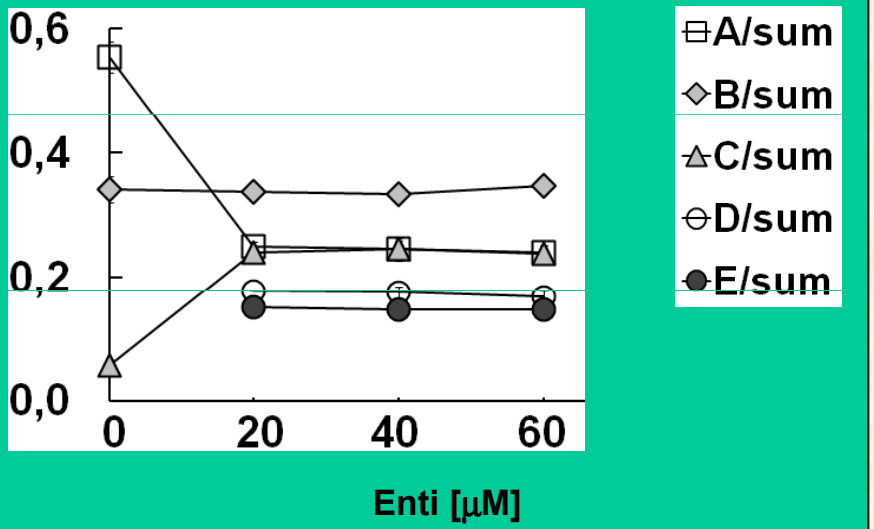

A → E 0 → 4 acetylations

Characterization of Post-Translational Modifications of Histones

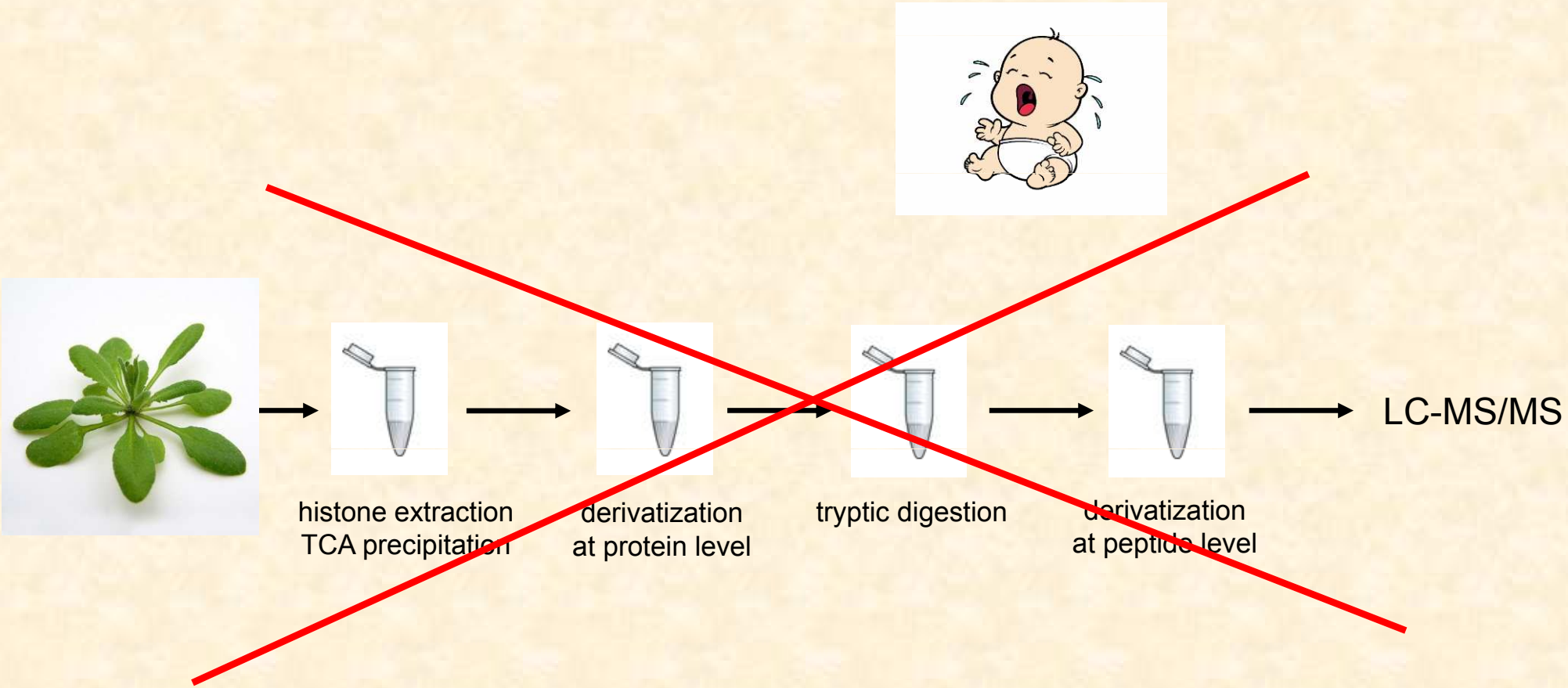

e.g. in Sidoli S. et al., J. Vis. Exp. 111:e54112 (2016).

Filter-Aided Sample Preparation Procedure for Mass Spectrometric Analysis of Plant Histones

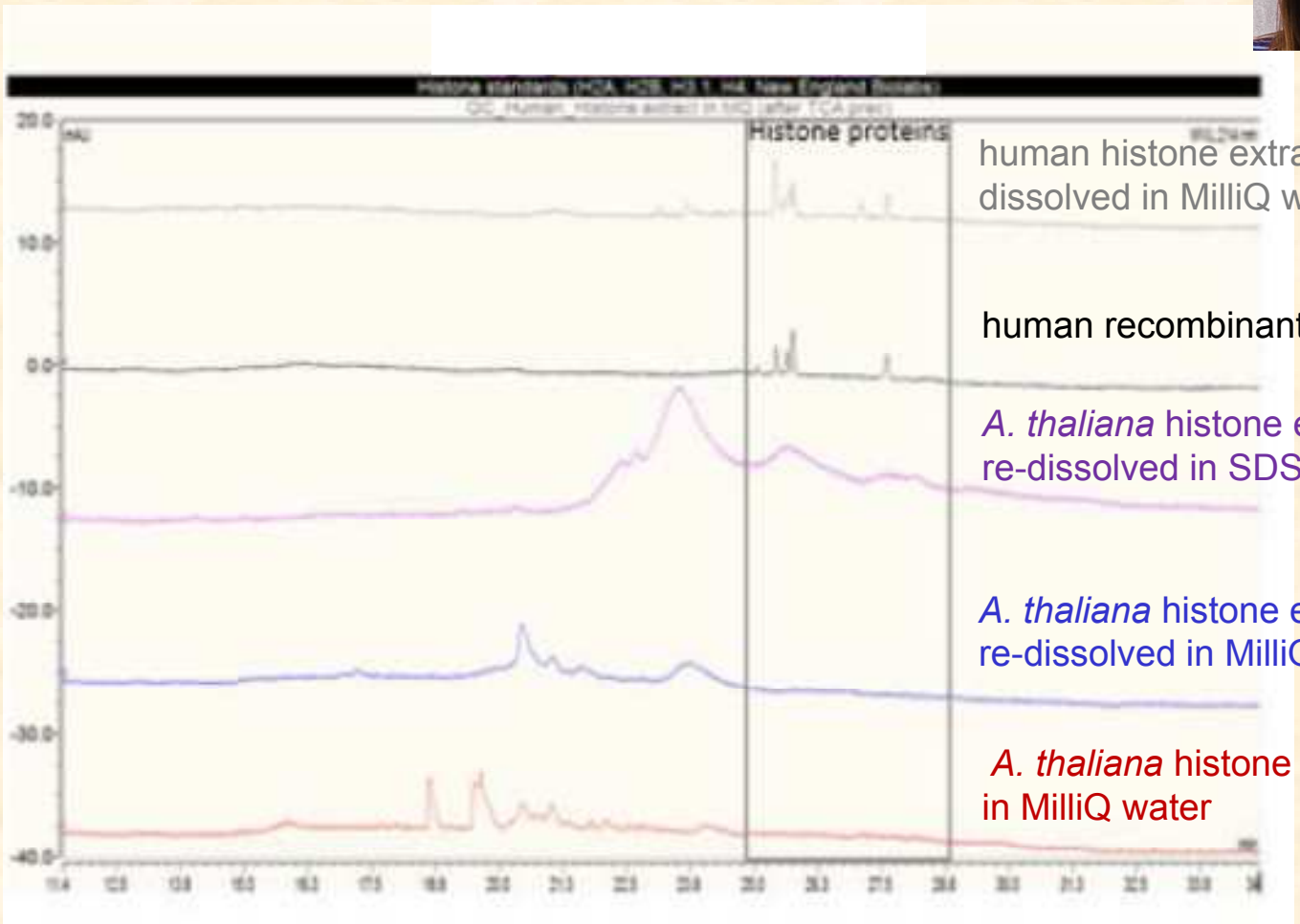

human histone extract after TCA precipitation re-dissolved in MilliQ water

human recombinant histone standards

A. thaliana histone extract after TCA precipitation re-dissolved in SDS

A. thaliana histone extract after TCA precipitation re-dissolved in MilliQ water

A. thaliana histone extract in sulfuric acid diluted in MilliQ water

Ledvinova D.. et al, Front. Plant Sci., ***9****, article 1373 (2018)*

Filter-Aided Sample Preparation Procedure for Mass Spectrometric Analysis of Plant Histones

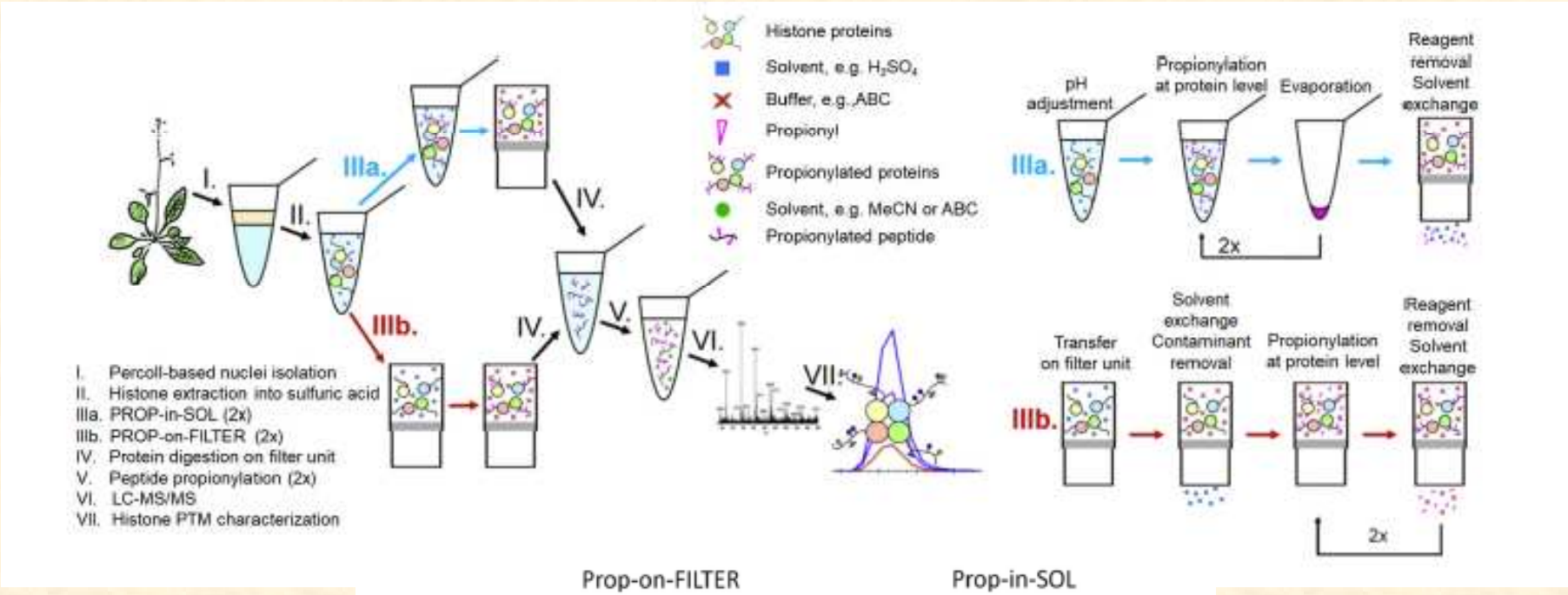

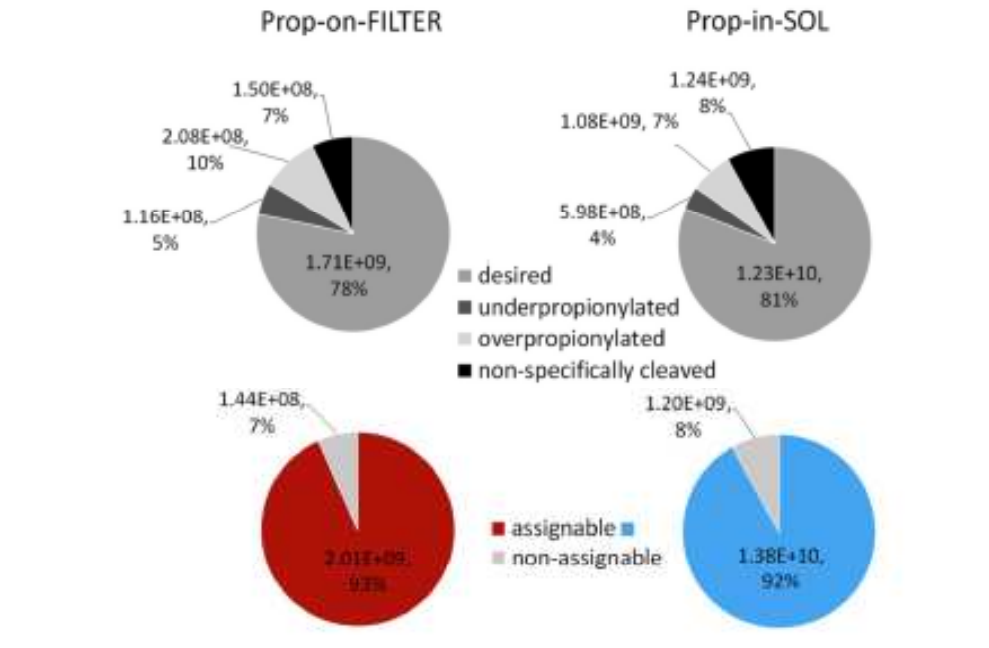

*Ledvinova D.. et al, Front. Plant Sci., **9**, article 1373 (2018)*

Inter-individual variations of Histone Modification Patterns

cooperation with Prof. Fajkus group, CEITEC-MU

two *Arabidopsis thaliana* ecotypes **Columbia 0** (Col-0) and **Wassilewskija** (Ws) grown from seeds collected from a **single parent plant** (Single) and a **set of parent plants** (Mixed).

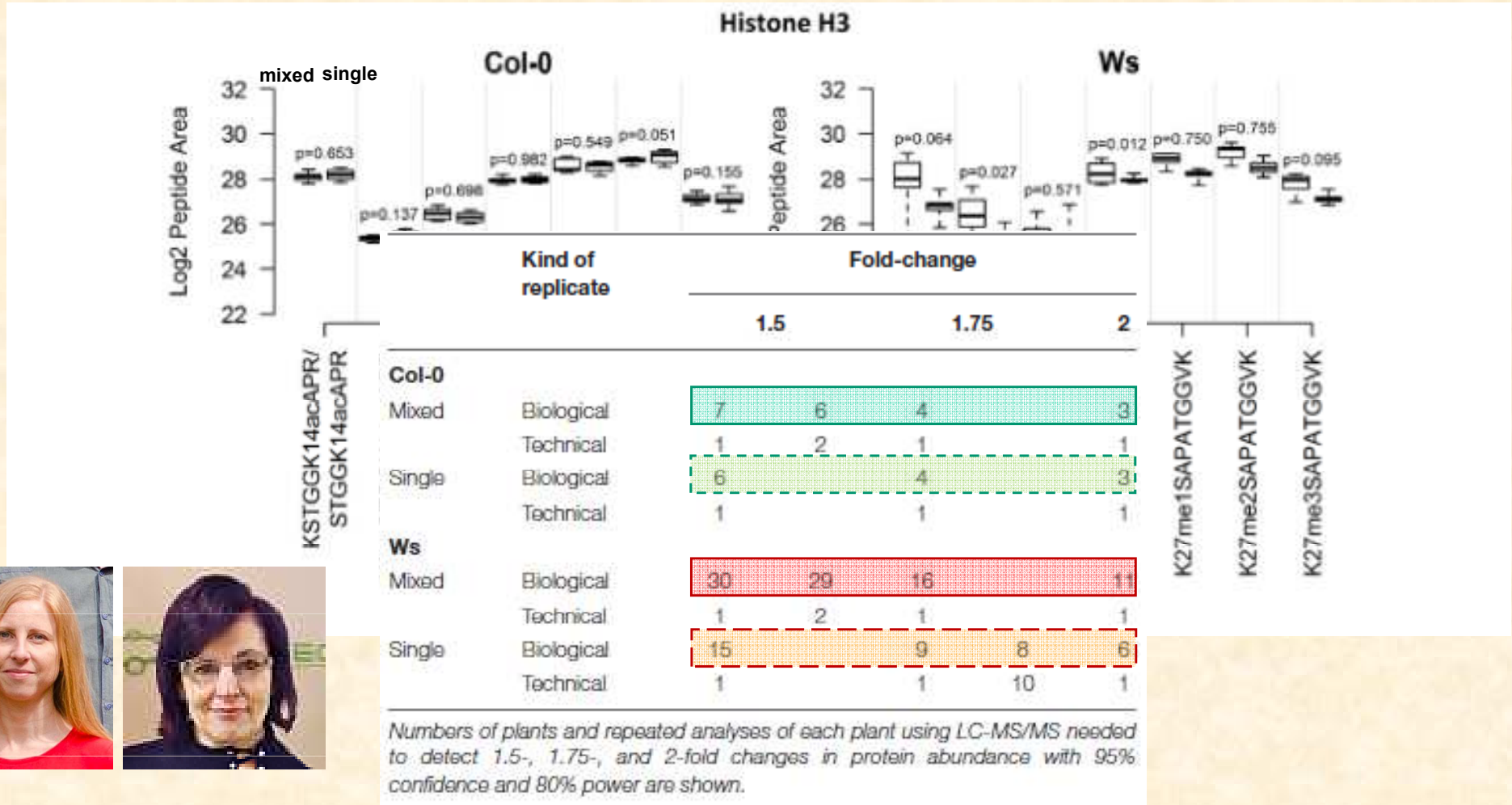

Numbers of plants and repeated analyses of each plant using LC-MS/MS needed to detect 1.5-, 1.75-, and 2-fold changes in protein abundance with 95% confidence and 80% power are shown.

*Brabencova S. et al, Front. Plant Sci., **8**, article 2084 (2017)*

Improvement of separation of histone peptide modified forms
novel derivatization agent

Histone H4 4-17 GKGGKGLGKGGAK

~ 2x more forms

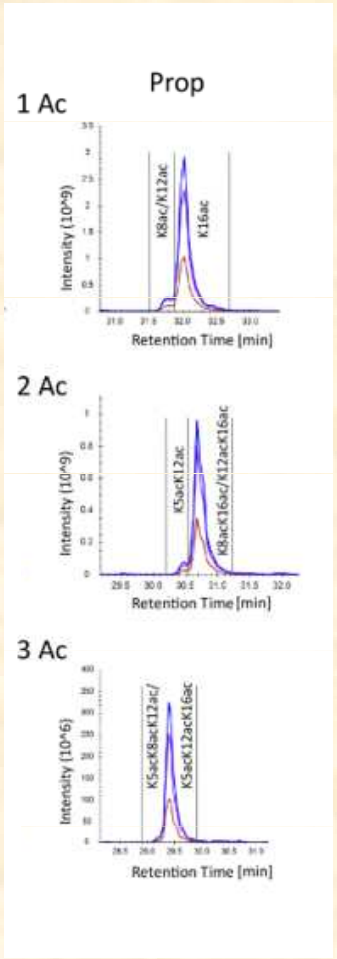

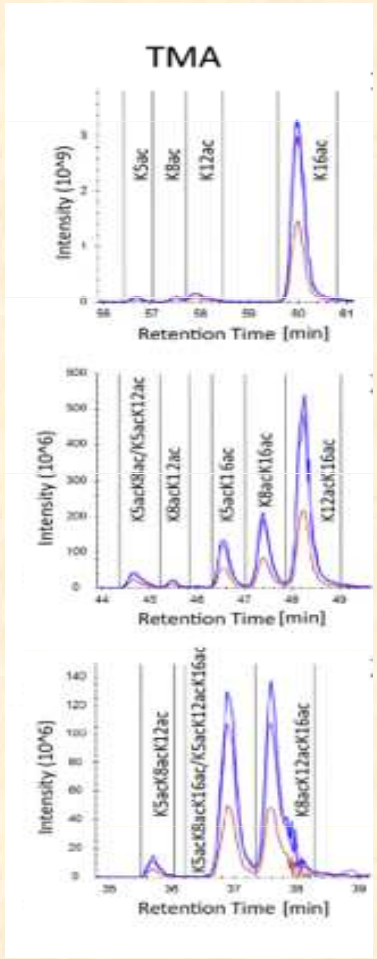

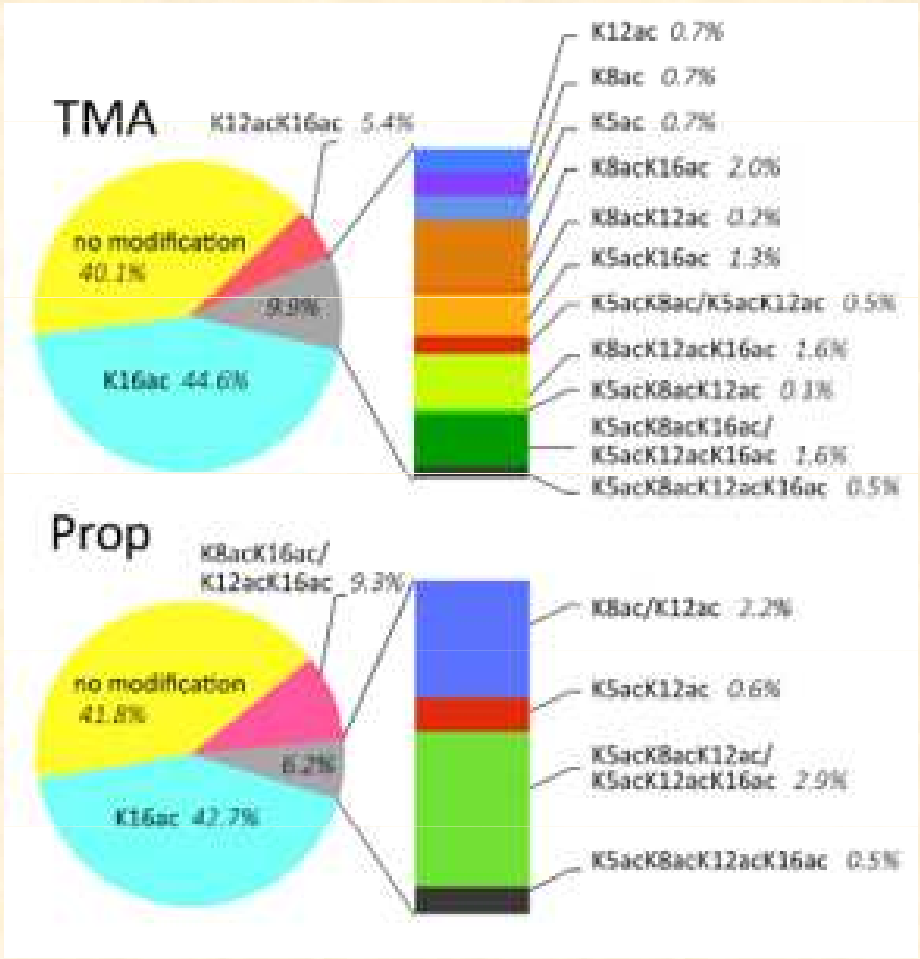

Histone extracts from MEC1 cell line.

Kucharikova et al, Mol. Cell. Proteomics, 20, 100114 (2021)

Assessment of effect of histone deacetylase inhibitors

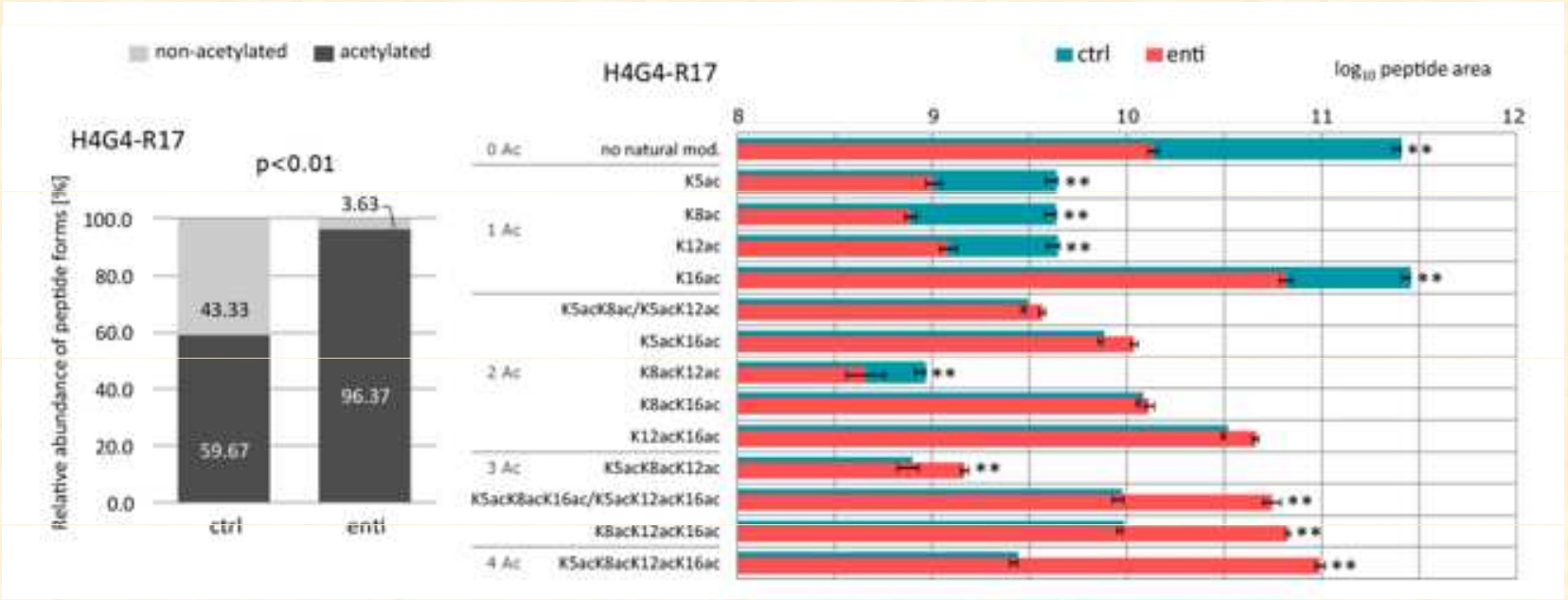

Kucharikova et al, Mol. Cell. Proteomics, 20, 100114 (2021)

HDAC inhibitors – potential for cancer treatment

Multi-level proteomics reveals host-perturbation strategies of SARS-CoV-2 and SARS-CoV

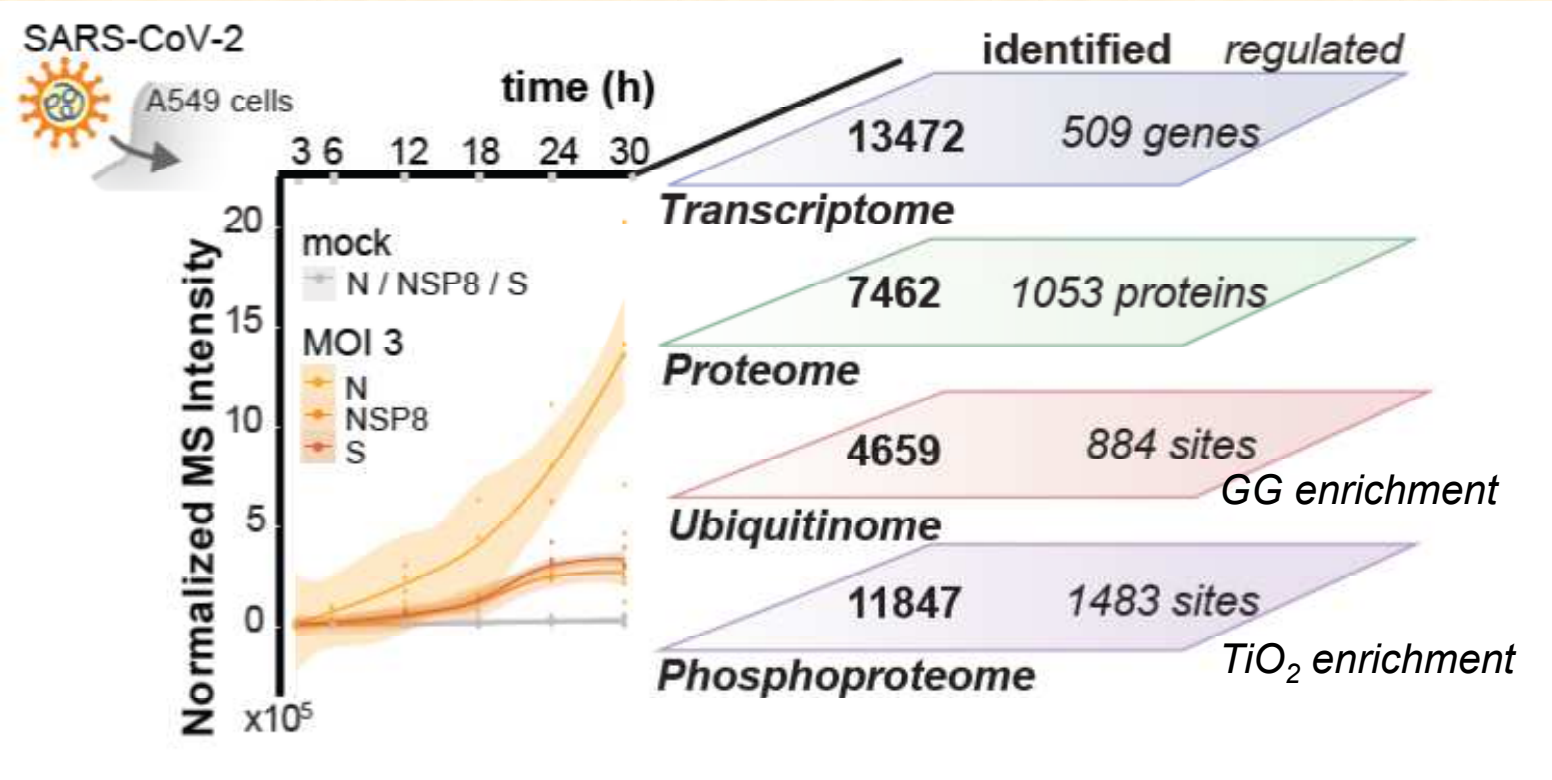

(a)Time-resolved profiling of SARSCoV-2 infection by multiple -omics methods. The plot shows normalized MS intensities of three SARS-CoV-2 viral proteins over time and overview of identified and regulated distinct transcripts, proteins, ubiquitination and phosphorylation sites, using data independent (DIA) or dependent (DDA) acquisition methods

Stukalov A. et al., bioRxiv: https://doi.org/10.1101/2020.06.17.156455


COPYRIGHT MARK H
AIRLINERS.NET

Charakterization of protein complexes
functional proteomics

- > 80% proteins is functional only as a part of complex
- ~ 10000 types of interactions

Aloy P., Russell R. B.: Nat. Biotechnol. ***22*** *(10), 1317-1321 (2004)*

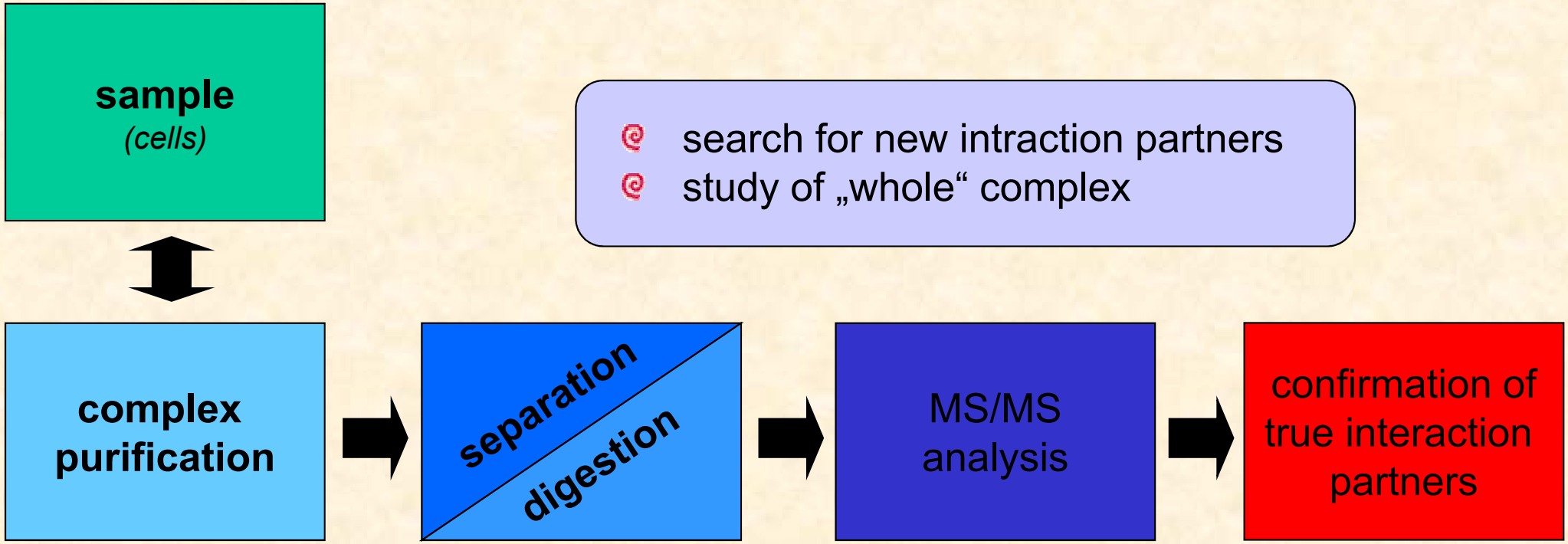

Purification of protein complexes

in vivo expression of bait protein with a tag

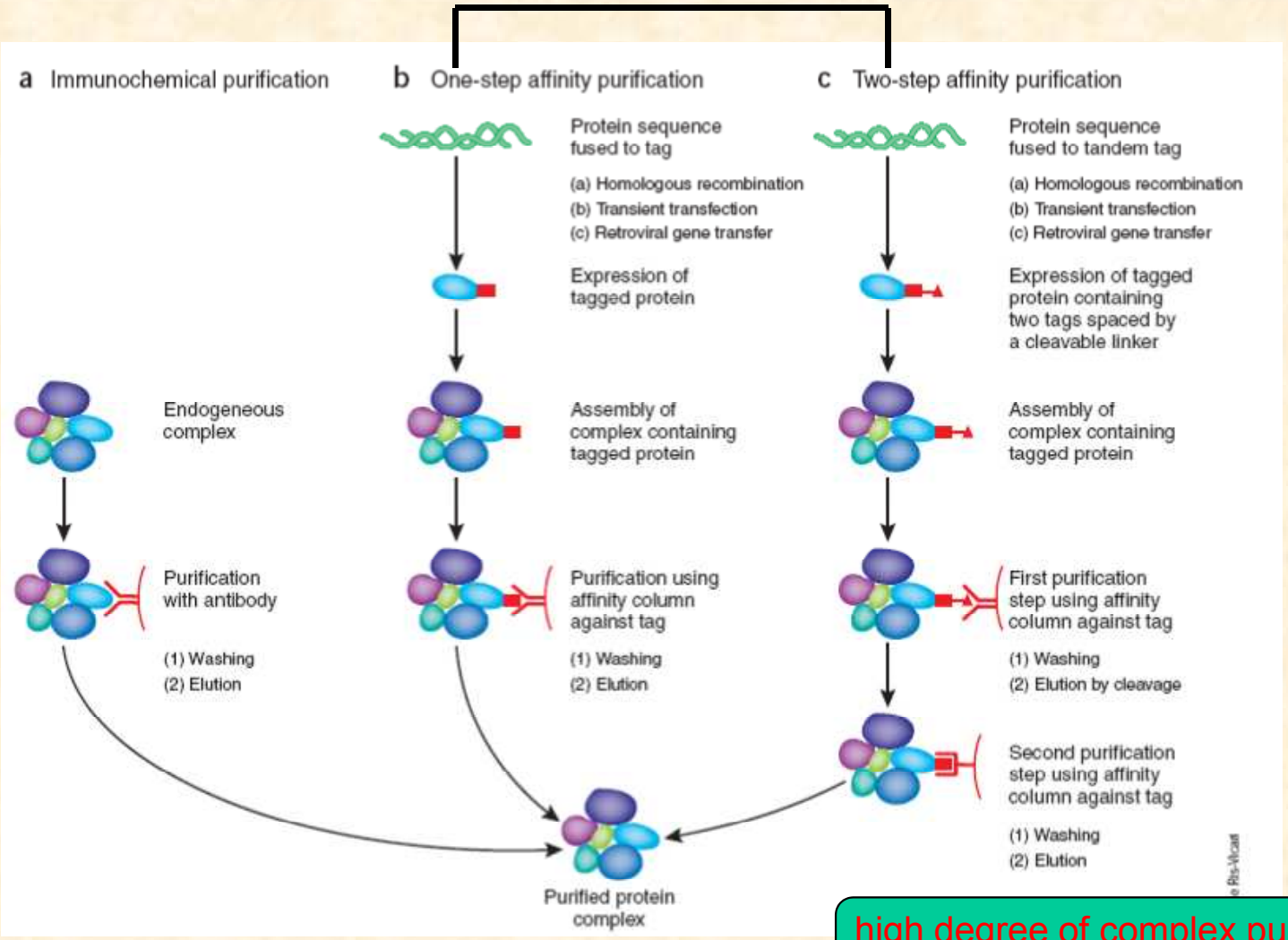

high degree of complex purity
loss of weakly binded interaction partners

*T. Köcher, G. Superti-Furga: Nat. Methods, **4**(10), 807-815 (2007).*

MS capabilities in protein complex analysis

- identification of individual complex members including their PTMs
- confirmation of interaction partners (exclusion of nonspecific interactors)
- determination of complex stoichiometry
- determination of 3D structure of complex (cross-linking)

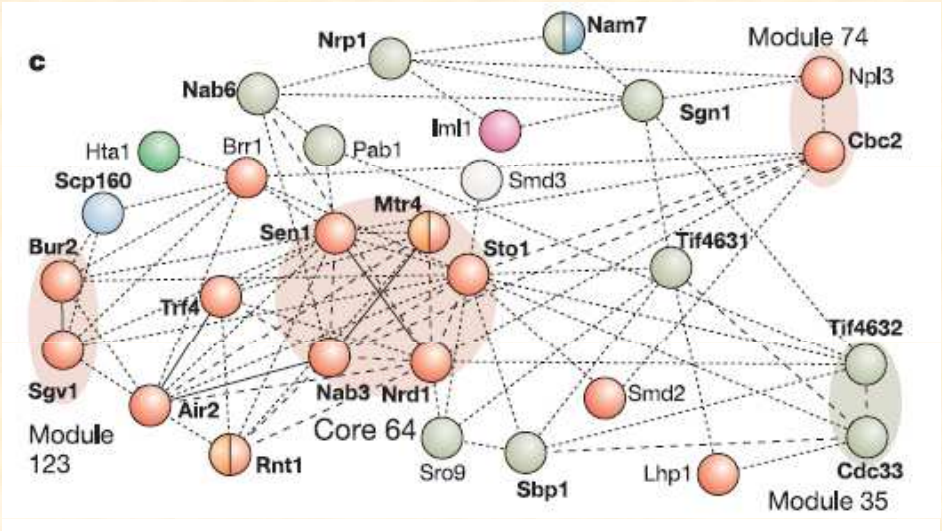

Gavin A.-C. et al.: Nature, **440** (30), 631-636.

Identification of individual interaction partners

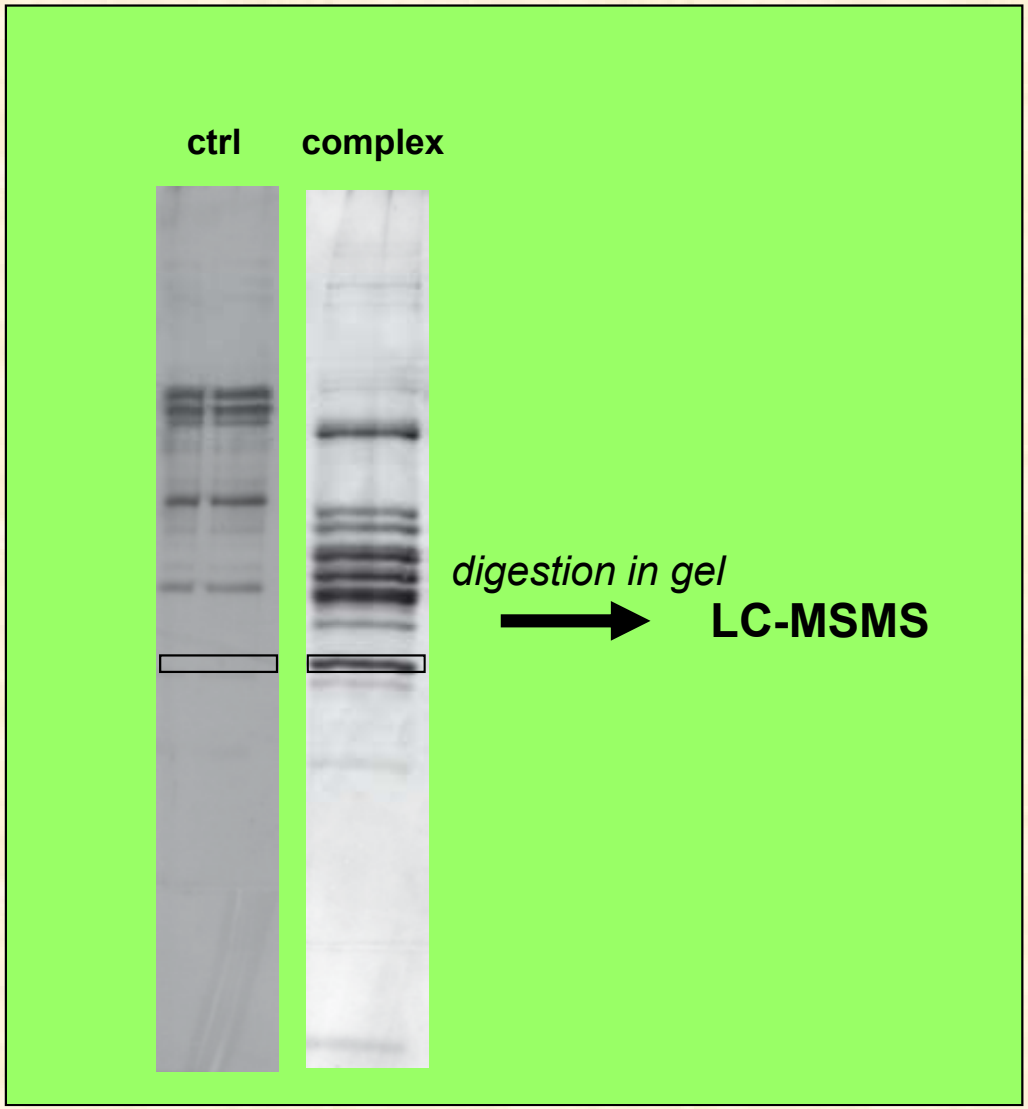

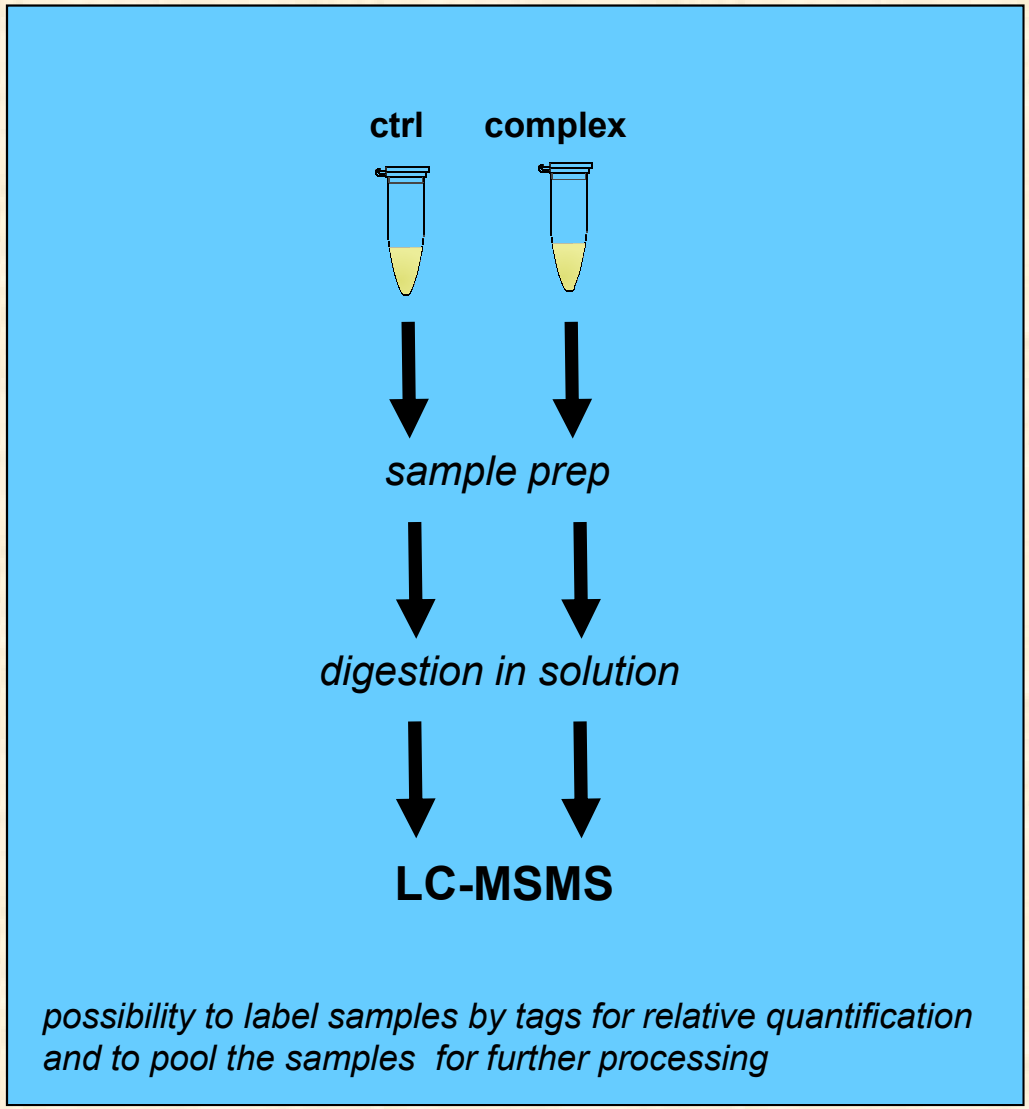

possibility to label samples by tags for relative quantification and to pool the samples for further processing

Confirmation of true interaction partners

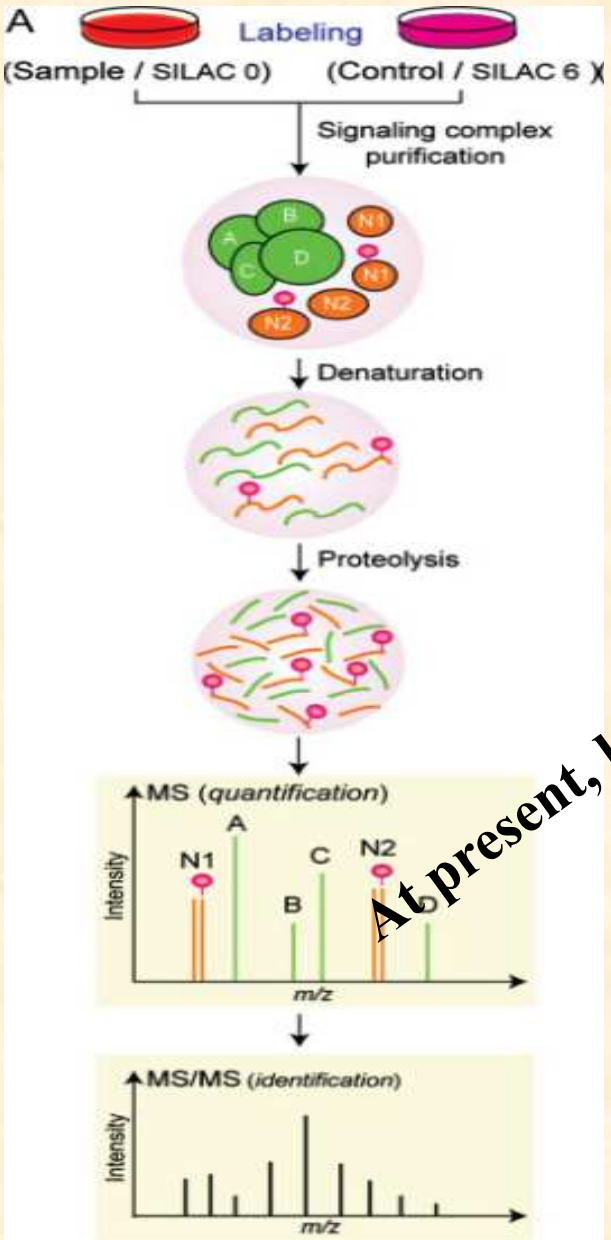

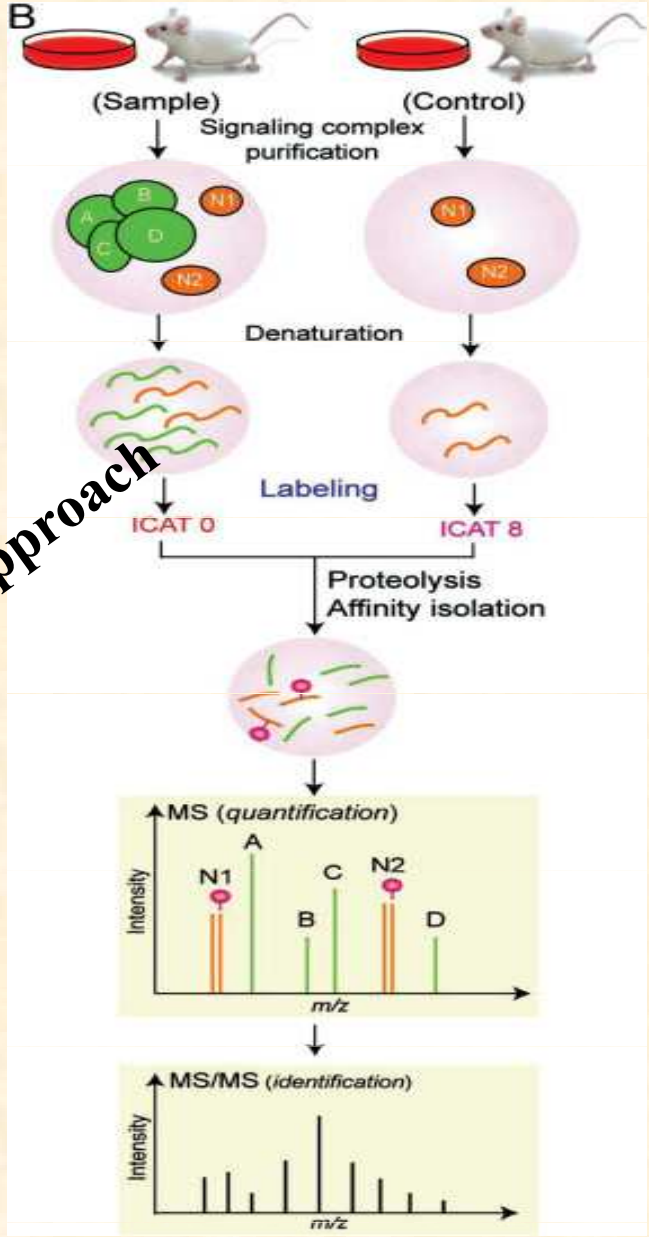

At present, label – free approach

non-specific interaction 1:1

W. Yang *et al., Proteomics* 2008, *8,* 832–851

Enzyme-catalyzed proximity labeling

BioID

unique method to screen for physiologically relevant protein interactions that occur in living cells.

Enzyme - **BirA** - the biotin protein ligase - of *Escherichia coli* biotinylates only a single cellular protein.

a mutant BirA attaches biotin to a large number of cellular proteins *in vivo*

Choi-Rhee E, Schulman H, Cronan JE. Protein Sci. 2004;13(11):3043–50

Enzyme-catalyzed proximity labeling

BioID

The **ligase is fused to a protein of interest** and expressed in cells, where it biotinylates proximal endogenous proteins.

Biotinylation is a rare protein modification in nature, it enables selective isolation and identification with standard **biotin-affinity capture.**

Proteins identified by BioID are candidate interactors for the protein of interest.

BioID can be applied to insoluble proteins, can identify **weak and/or transient interactions**, and is amenable to temporal regulation.

Initially applied to mammalian cells, BioID has potential application in a variety of cell types from diverse species.

Roux KJ, Kim DI, Burke B. Curr Protoc Protein Sci. 2013;74:Unit 19 23.

Enzyme-catalyzed proximity labeling

BioID

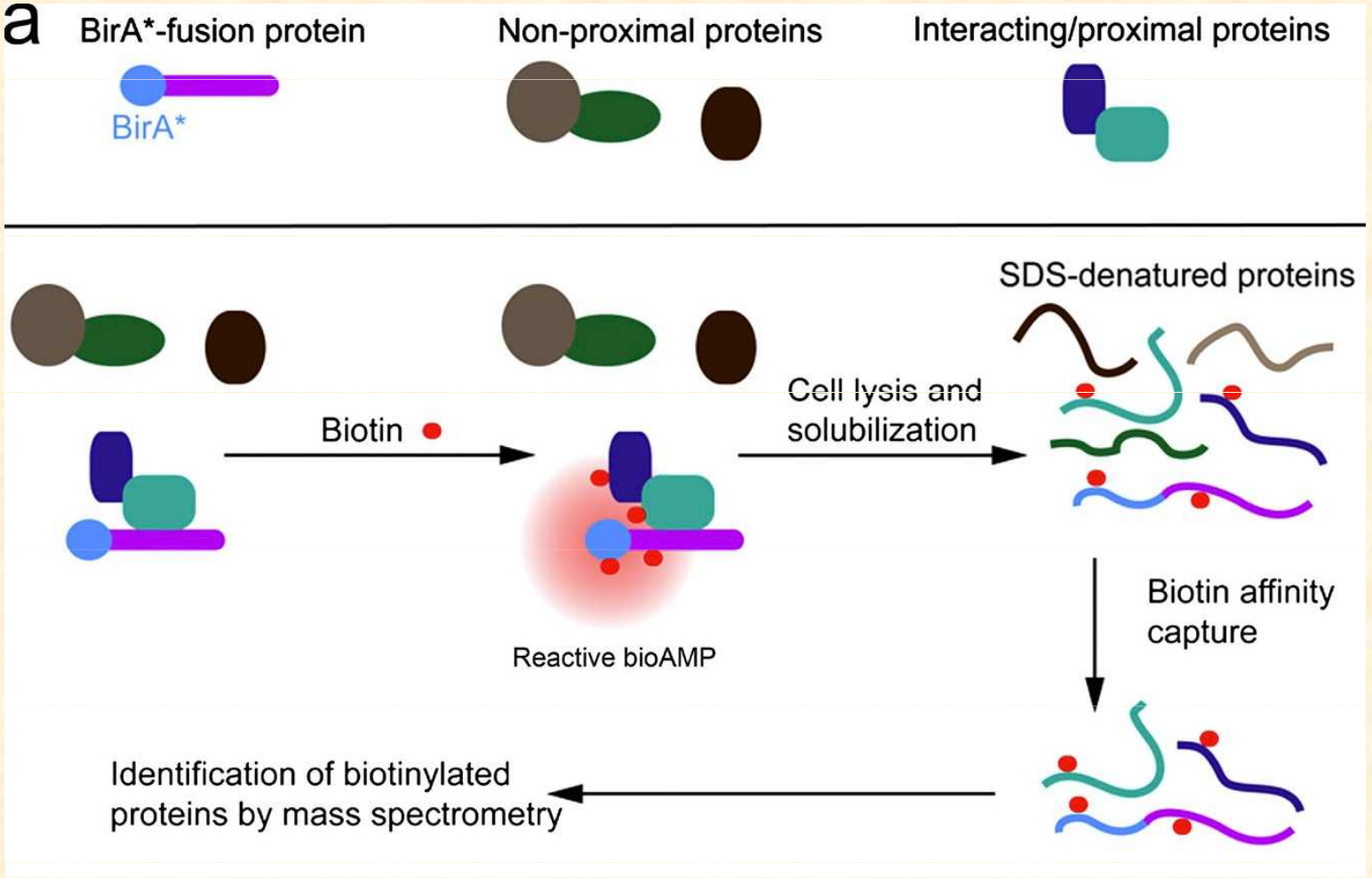

Roux KJ, Kim DI, Raida M, Burke B. J Cell Biol. 2012;196(6):801–10

Enzyme-catalyzed proximity labeling

TurboID/miniTurbo

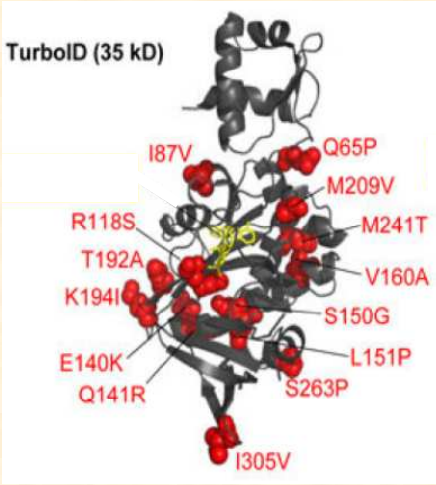

- multiply mutated BirA
- higher efficiency of labeling than BioID or BioID2
- faster kinetics

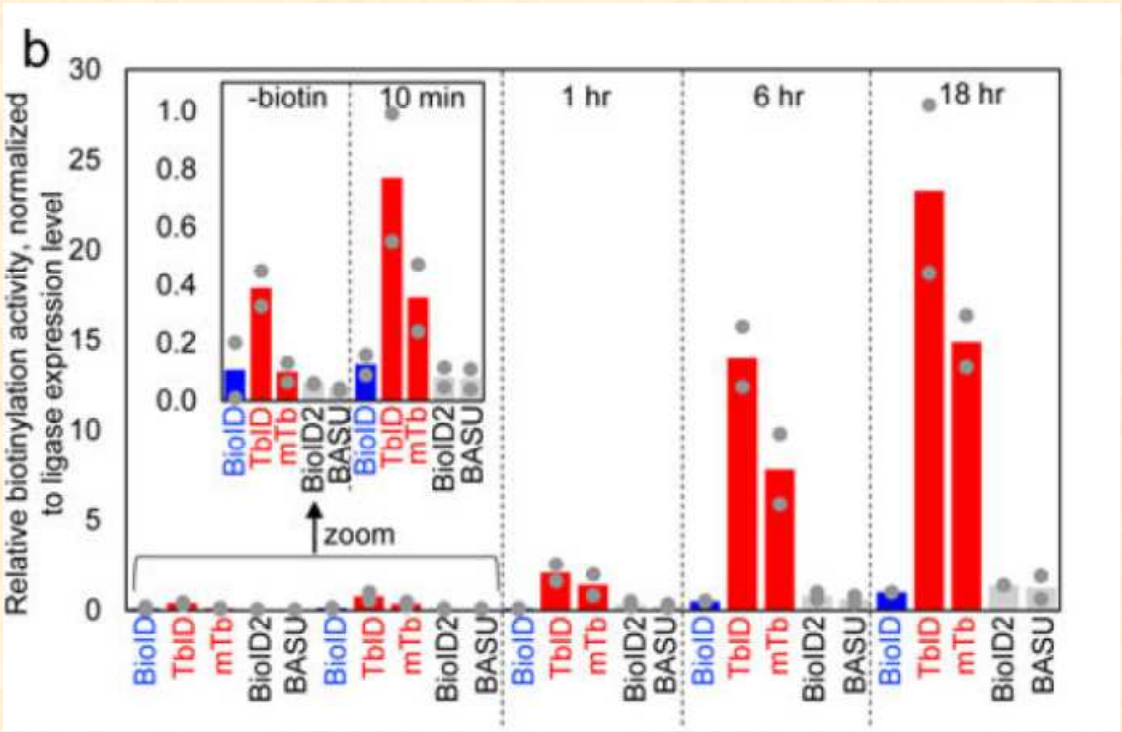

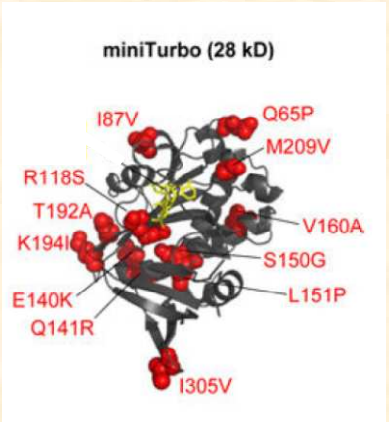

Branon T., C. et al., Nat Biotechnol. 2018 October ; 36(9): 880–887


WIENER PHILHARMONIC
Austrian
COPYRIGHT ANDY GRAF
AIRLINERS.NET

Sequence confirmation and determination of OBP protein isoforms

de novo sequencing

Myodes glareolus

- saliva
- 2D gel electrophoresis
- MS/MS of selected spots

- unknown genome
- no antibodies

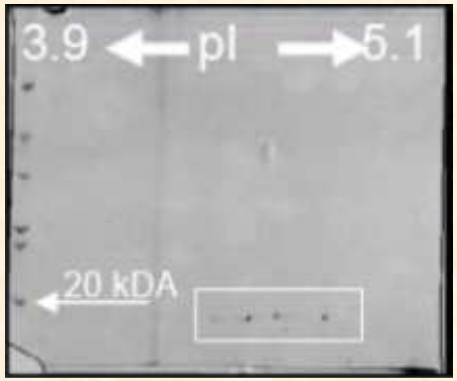

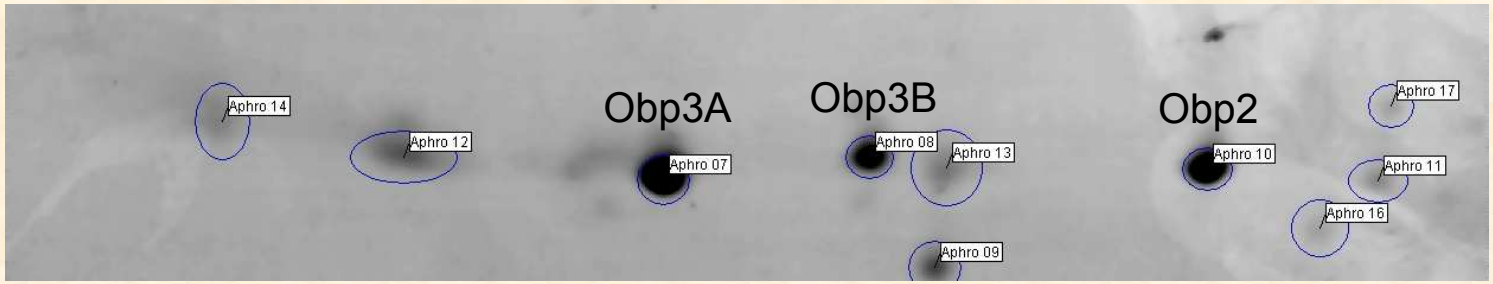

cooperation with prof. Stopka FS CU, Prague

*Stopková R., Zdráhal Z., Ryba Š. et al, BMC Genomics 2010, **11**:45*

Sequence confirmation and determination of OBP protein isoforms

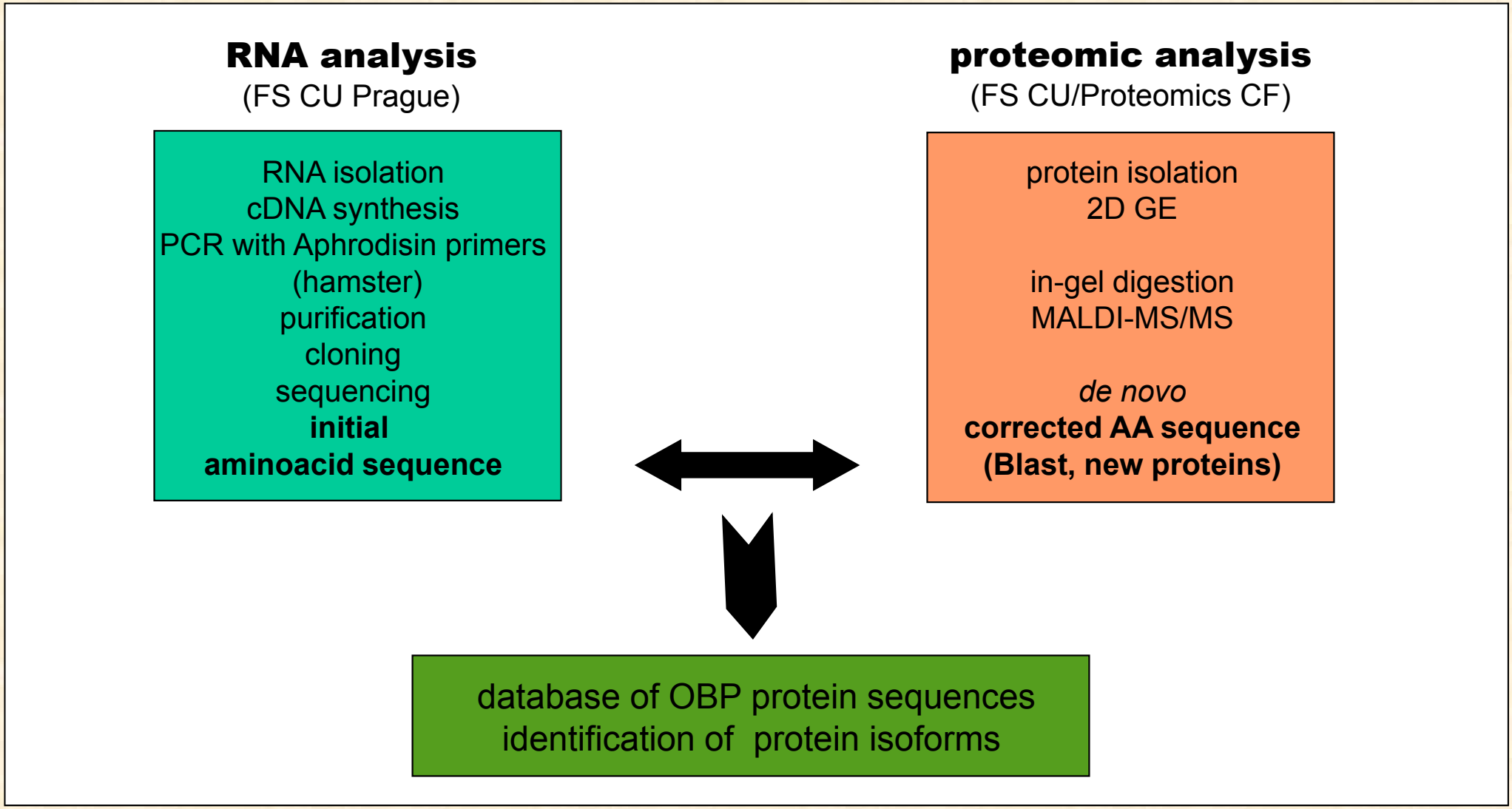

Sequence confirmation and determination of OBP protein isoforms

MALDI-MS/MS a LC-MS/MS
manual spectra interpretation

original sequence - QAELEGKWVTTAIAADNIDTIEEEGPMR (OBP3)

DAELEGTWYTTAIAADNVDTIEEEGPLR

HAELEGTWYTTAIAADNVDTIEEEGPLR

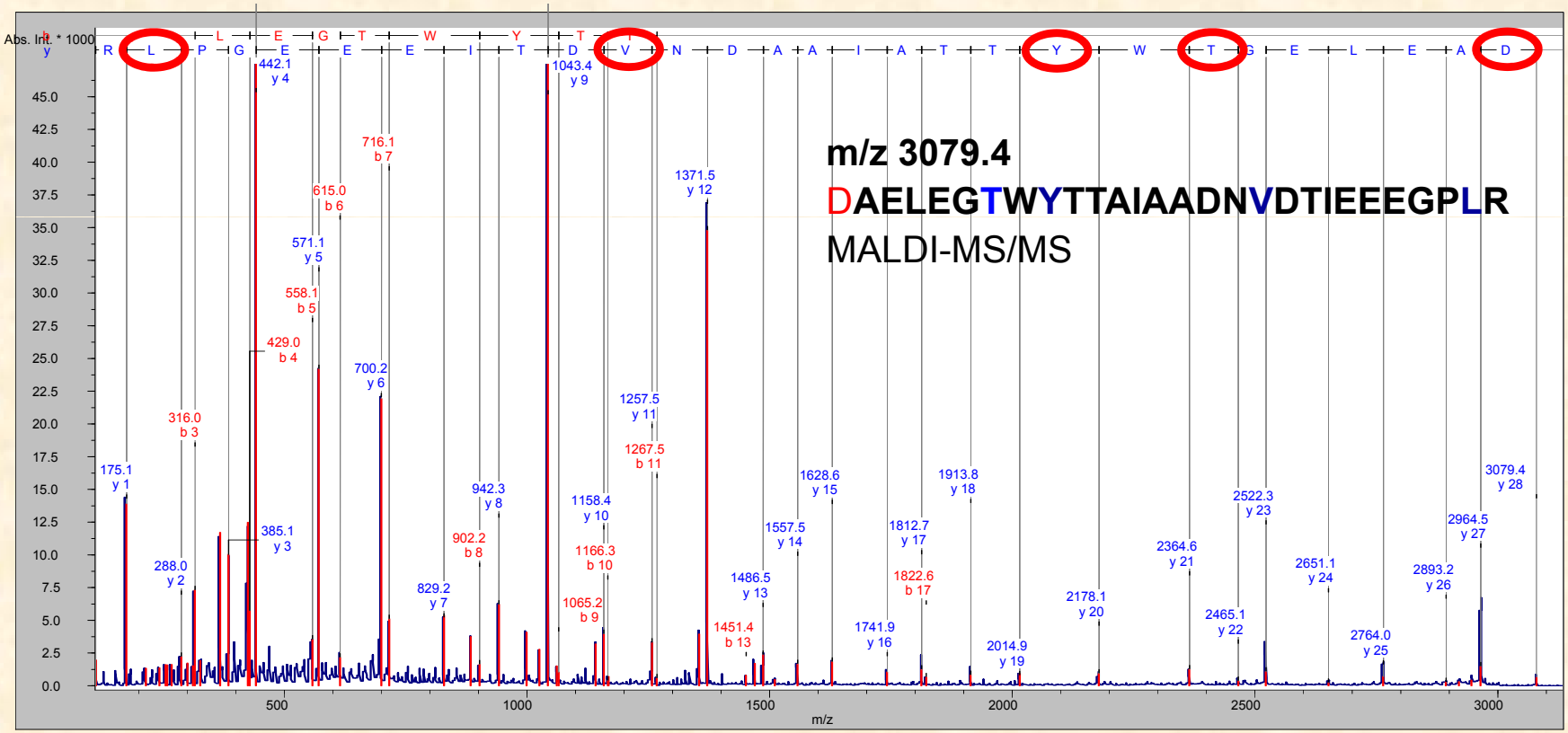


JAL
JAL DREAM EXPRESS
912
Photo Copyright Avibear
AIRLINERS.NET

MS Imaging

MALDI-MS imaging

samples:

- fresh frozen tissue sections
- individual cells or clusters of cells isolated by **laser-capture microdissection** or **contact blotting** of a tissue on a membrane target.

MS analysis

- scanning of sample area point by point
- image corresponds to planar distribution of individual *m/z*

distribution of peptides (proteins, lipids,...)

MALDI-MS imaging

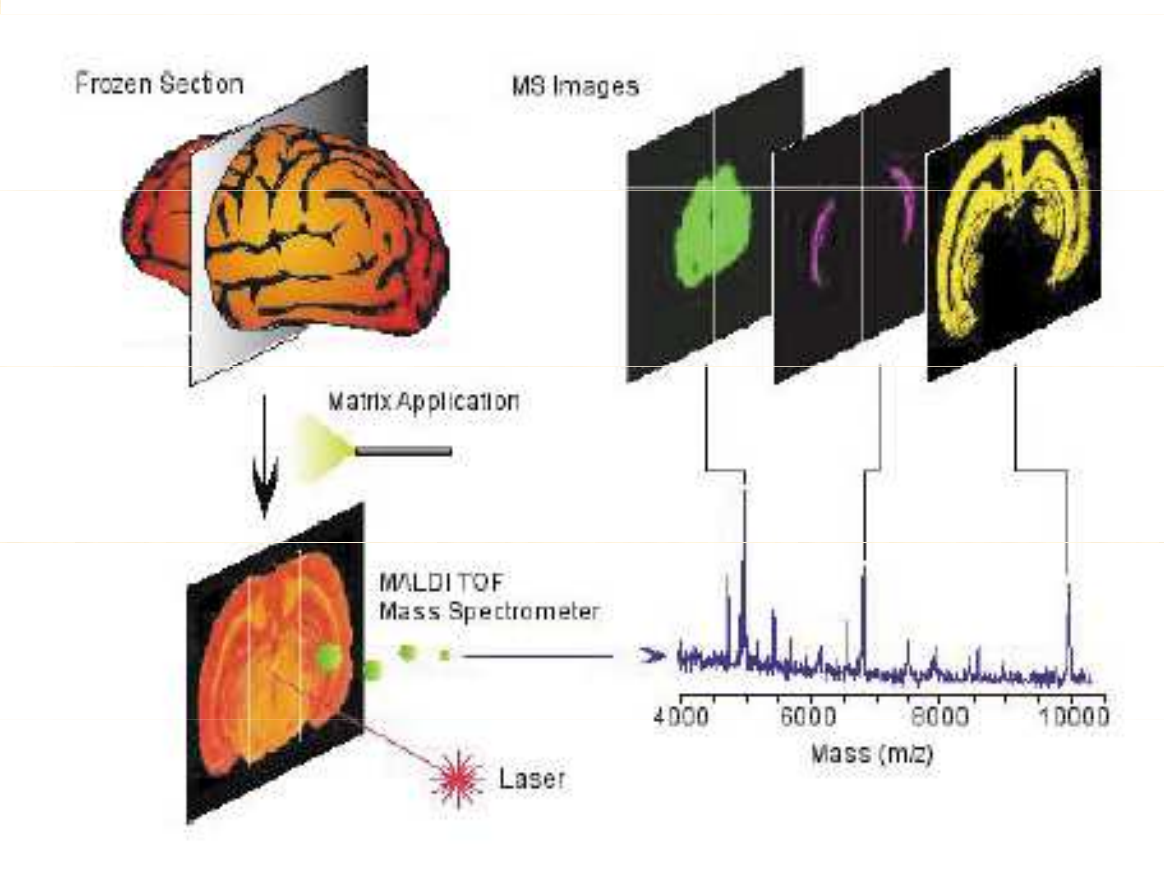

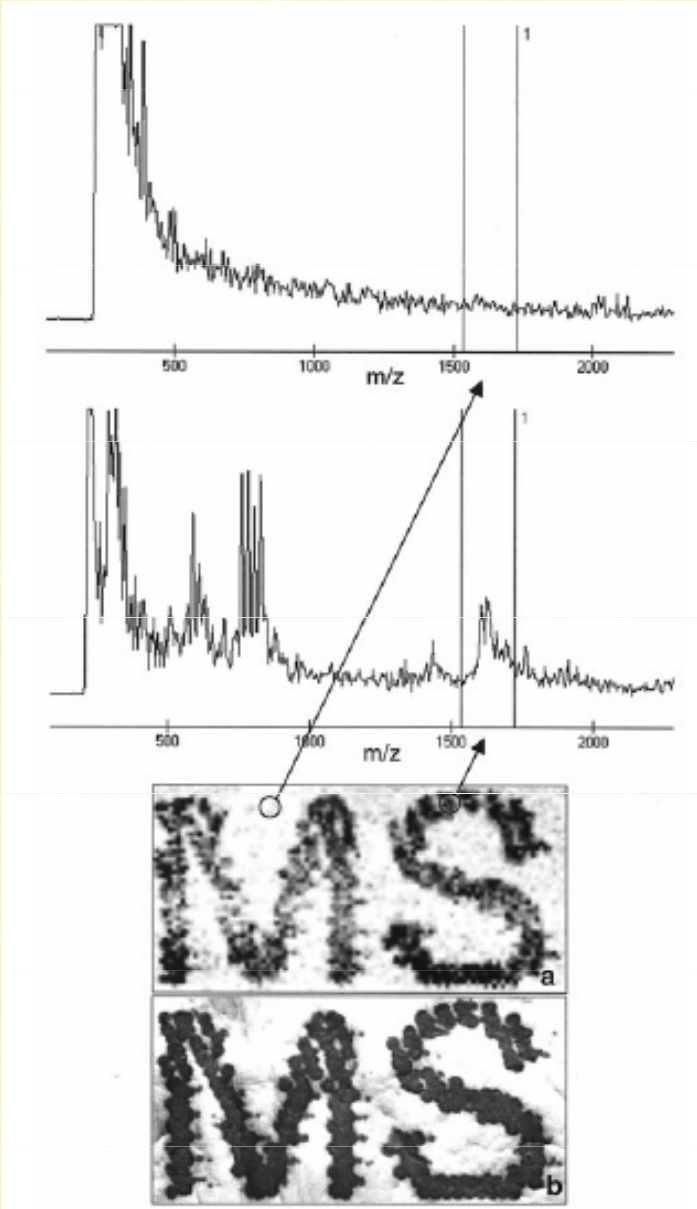

Figure 3. Neurotensin was added to the ink of a printer. The mass spectrometry image (a) (100 × 50 pixels, 3 × 1.5 mm) obtained of the protonated neurotensin peak matches with the optical image (b).

M. Stoeckli, T.B. Farmer, R.M. Caprioli: *J Am Soc Mass Spectrom*, **10**, 67–71 (1999)

MALDI-MS imaging

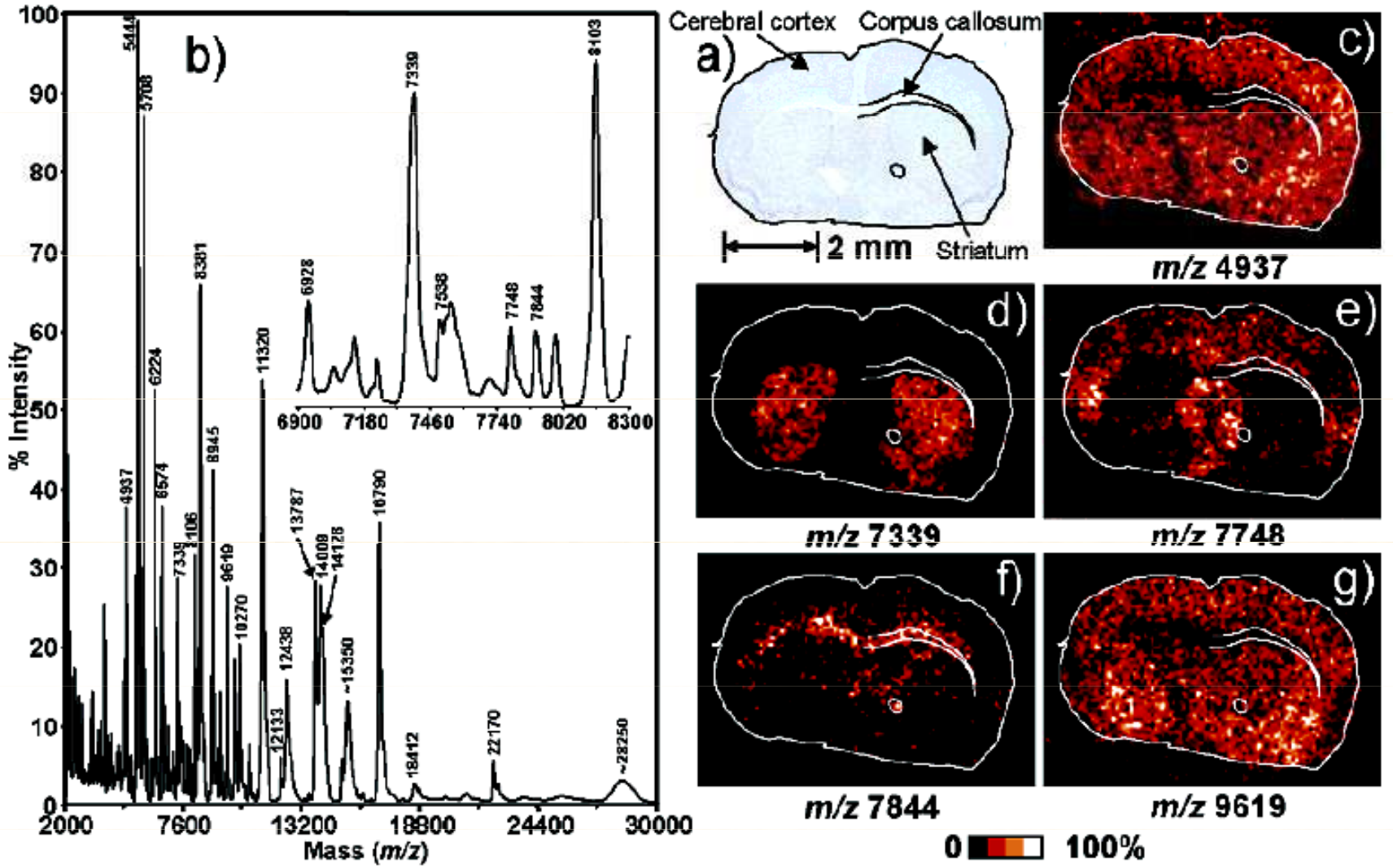

Figure 8. IMS analysis of a 12-μm coronal mouse brain section. (a) Photomicrograph of a Cresyl Violet-stained section showing different anatomic brain substructures. (b) MALDI-MS protein profile obtained after homogeneous matrix deposition averaging all of the individual spectra acquired from the section. (c–g) Ion density maps obtained at different *m/z* values with an imaging resolution of 100 μm. The ion density maps are depicted as pseudocolor images with white representing the highest protein concentration and black the lowest.

Chaurand *et al*:*Anal. Chem.***2004,** 76,1145-1155

Degradation of Ang III and Ang-(1–7) in mouse kidney sections.

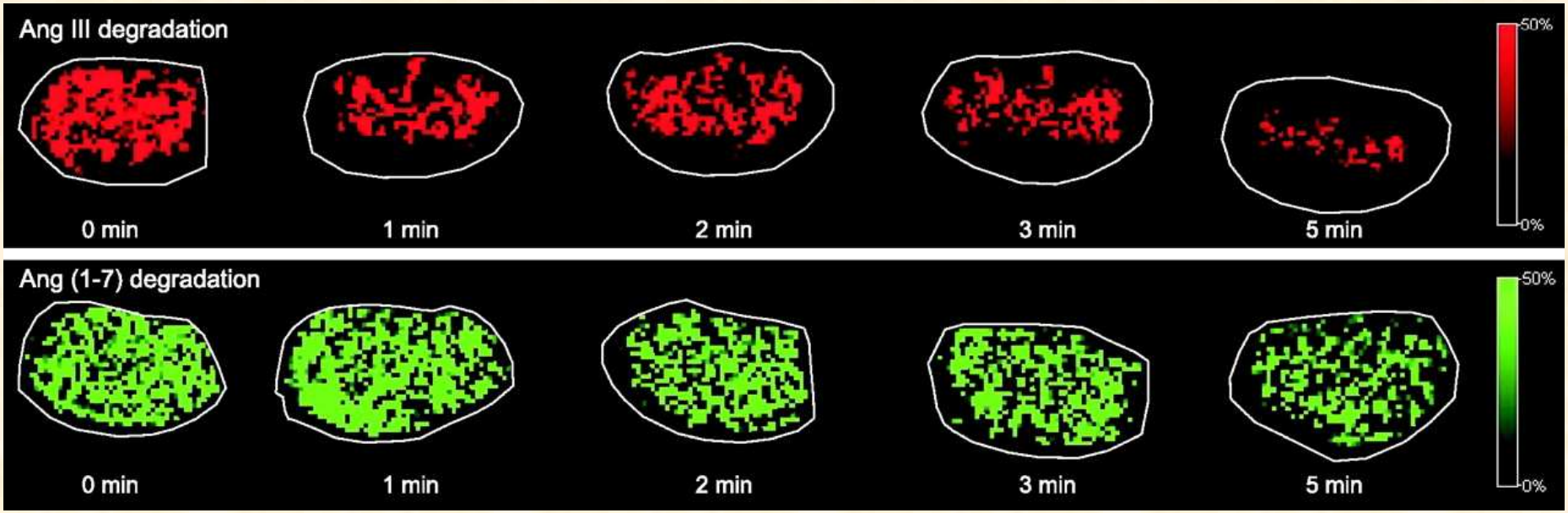

Grobe N. et al, Am. J. Physiol. Endocrinol. Metab., 302 (8), E1016 (2012)

SpatialOMx Workflow

SpatialOMx is the combination of using MALDI Imaging and ESI to unlock a 5th dimension and show the distribution of target compounds. On the timsTOF fleX, use the MALDI source to map the distribution of molecules in your sample and identify regions of interest. After extracting and preparing the sample for LCMS, use the ESI source for the highest level of identifications

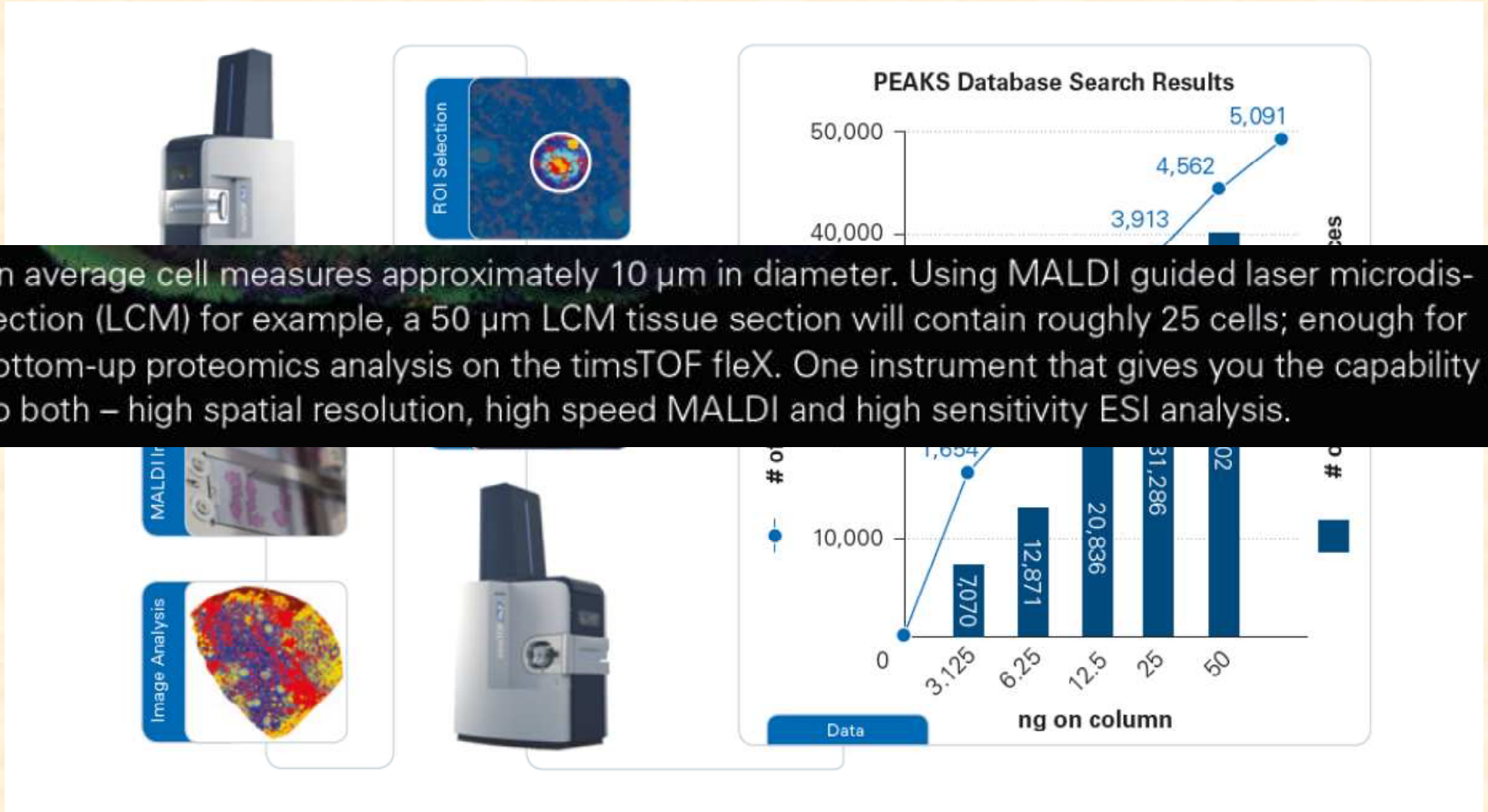

An average cell measures approximately 10 µm in diameter. Using MALDI guided laser microdissection (LCM) for example, a 50 µm LCM tissue section will contain roughly 25 cells; enough for bottom-up proteomics analysis on the timsTOF fleX. One instrument that gives you the capability to do both – high spatial resolution, high speed MALDI and high sensitivity ESI analysis.

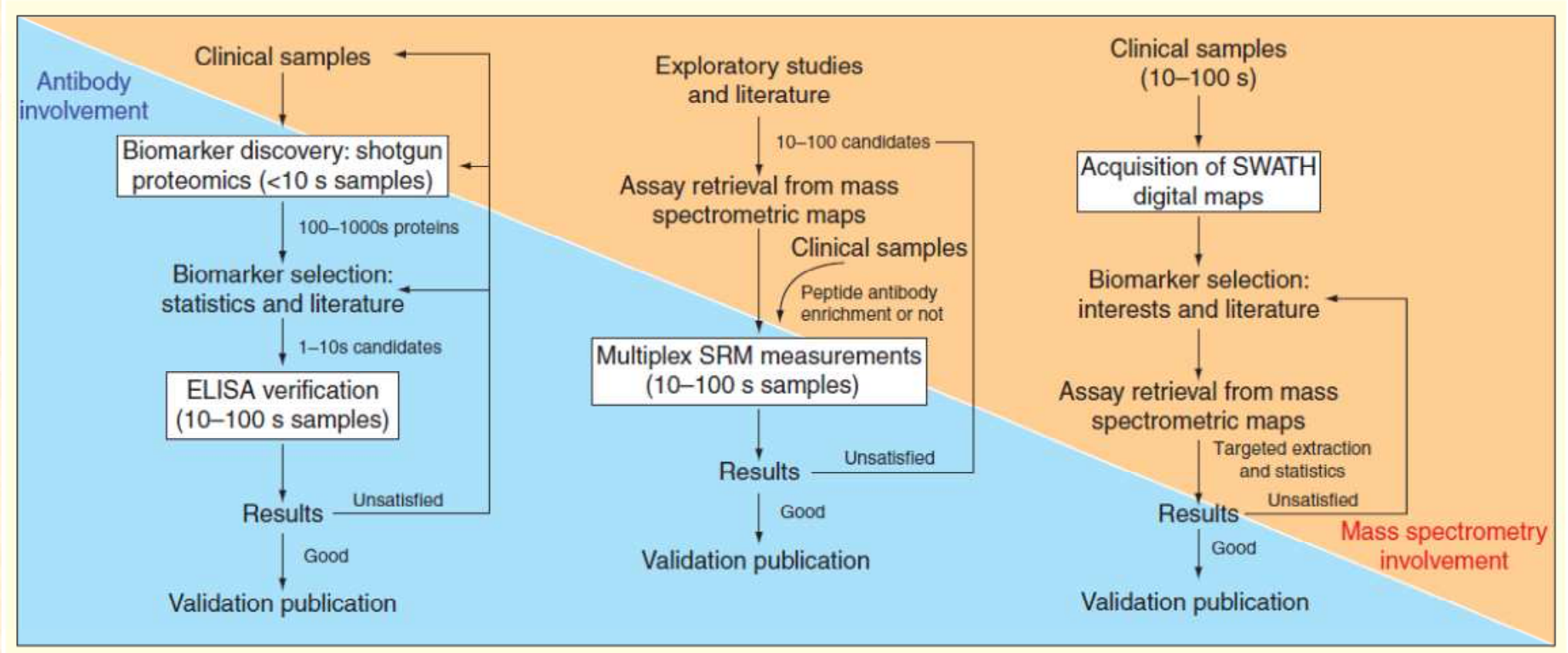

Liu et al, Expert Rev. Mol. Diagn., 13(8), 811 (2013)


VFA-14
202

Nanopore peptide sequencing

A DNA-peptide conjugate was pulled through the biological nanopore MspA by the DNA helicase Hel308. Reading the ion current signal through the nanopore enabled discrimination of single–amino acid substitutions in single reads.

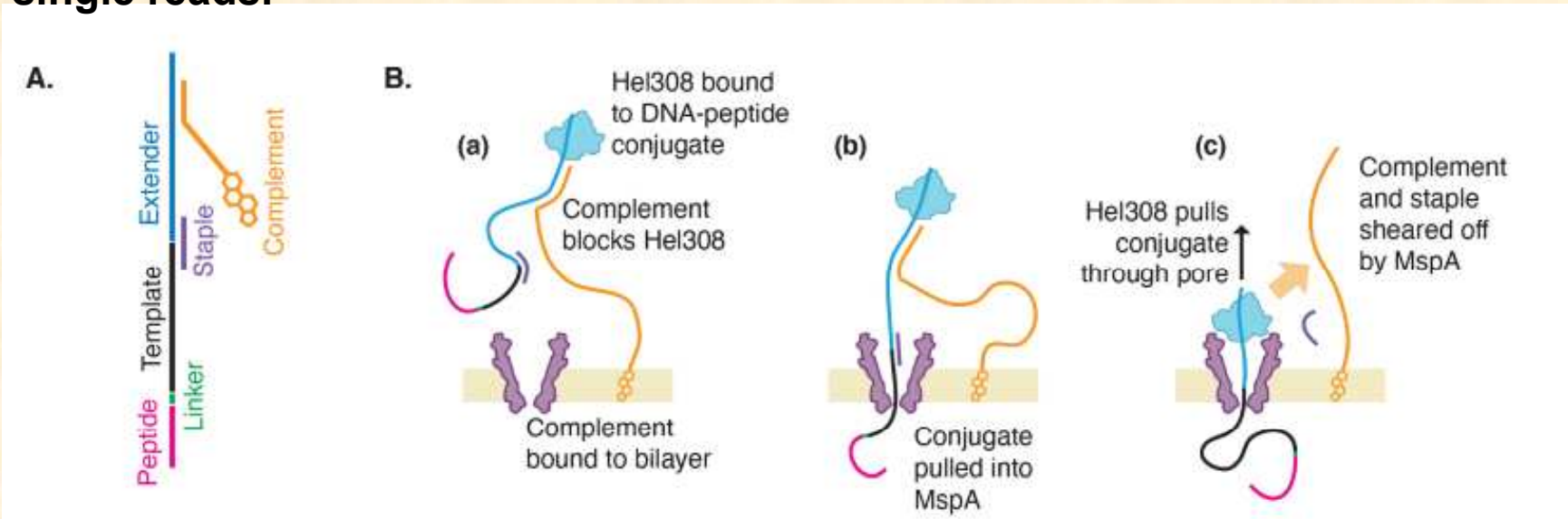

Fig. 1. Reading peptides with a nanopore.
A) The DNA-peptide conjugate consists of a peptide (pink) attached via a click linker (green) to an ssDNA strand (black). This DNA-peptide conjugate is extended with a typical nanopore adaptor comprised of an extender that acts as a site for helicase loading (blue) and a complementary oligo with a 3′ cholesterol modification (gold).
B) The cholesterol associates with the bilayer as shown in (a), increasing the concentration of analyte near the pore. The complementary oligo blocks the helicase, until it is pulled into the pore (b), causing the complementary strand to be sheared off (c), whereupon the helicase starts to step along DNA.

H. Brinkerhoff et al., Science 10.1126/science.abl4381 (2021)

Nanopore peptide sequencing

(**C**) As the helicase walks along the DNA, it pulls it up through the pore, resulting in (a) a read of the DNA portion followed by (b) a read of the attached peptide.

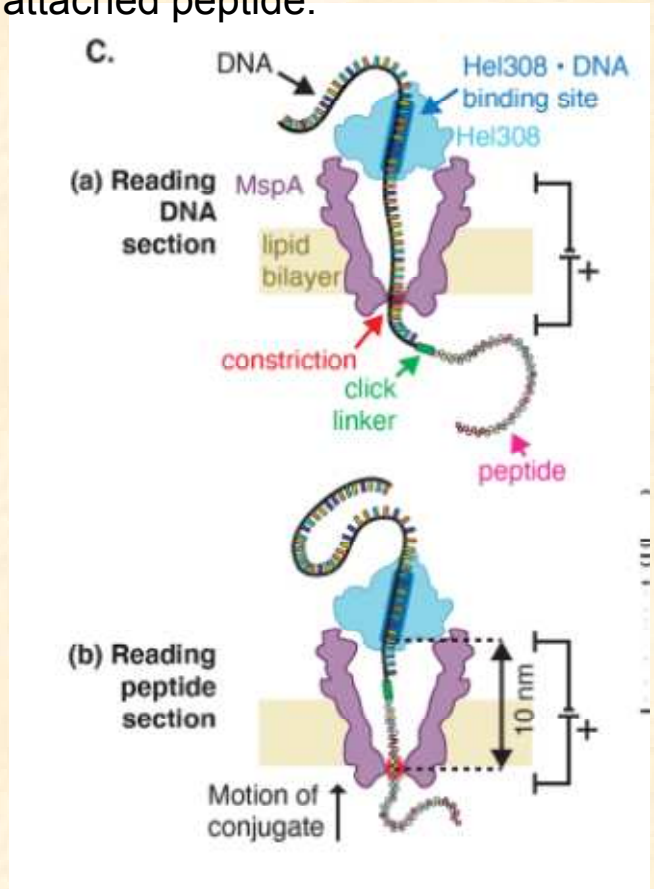

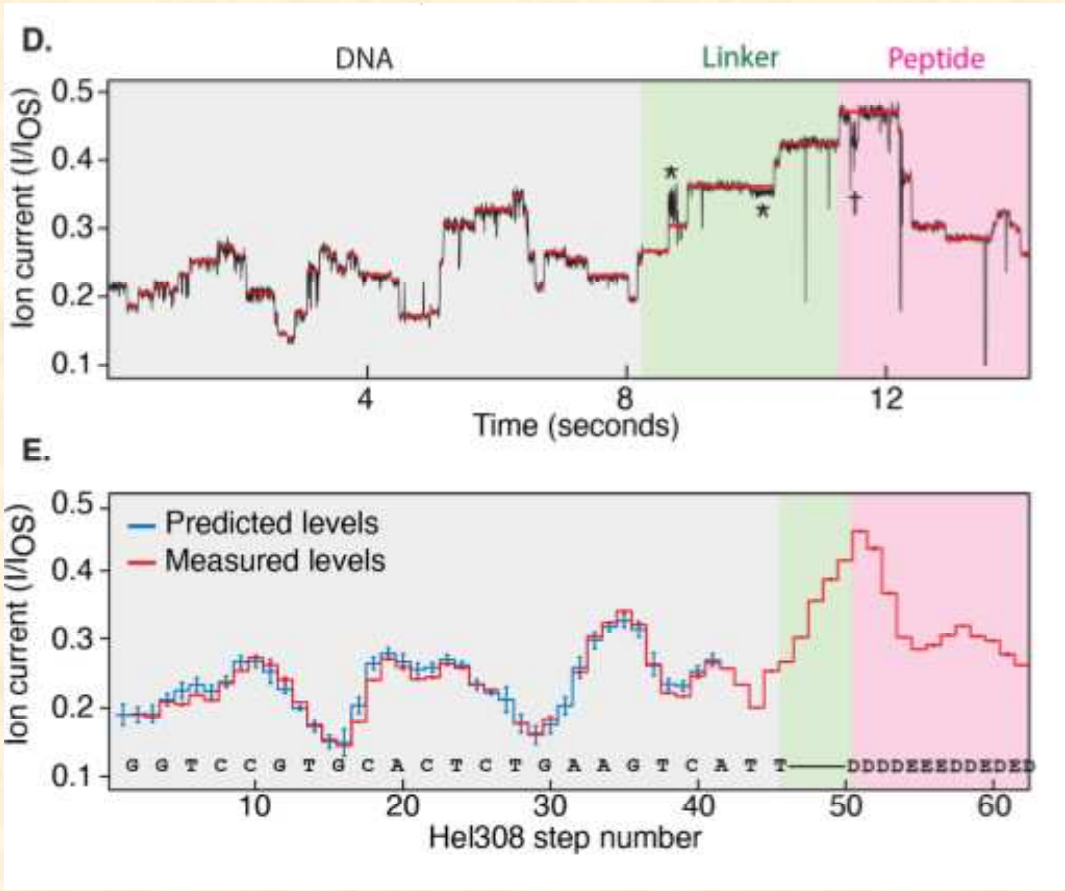

(**D**) Typical nanopore read of a DNA-peptide conjugate (black), displaying step-like ion currents (identified in red). The asterisks * indicate a spurious level
not observed in most reads and therefore omitted from further analysis. The dagger † indicates a helicase backstep. (**E**) Consensus sequence of ion current steps (red), which for the DNA section is closely matched by the predicted DNA sequence (blue). The linker and peptide sections are identified by counting half-nucleotide steps over the known structural length of the linker. Error bars in the measured ion current levels are errors in the mean value, often too small to see.

H. Brinkerhoff et al., Science 10.1126/science.abl4381 (2021)

The end